PHYSICAL REVIEW B VOLUME 25, NUMBER 3 1 FEBRUARY 1982

NMR evidence for an ionic model of Cr, Mn, and Fe in Cu

Daniel C. Abbas,* Thomas J. Aton,† and Charles P. Slichter
Department of Physics and Materials Research Laboratory, University of Illinois at Urbana-Champaign, Urbana, Illinois 61801
(Received 2 July 1981)

The authors have found that the NMR frequencies of Cu atoms which are near neighbors to Cr atoms in dilute *Cu*Cr have an anomalous temperature dependence, in contrast with *Cu*Mn and *Cu*Fe which display the usual form governed by a Curie-Weiss law. The authors show that all the data can be explained by an ionic model of the magnetic impurity which assumes a definite $3d^n$ configuration with a definite *L-S* ground state and includes intraconfigurational energy-level splittings due to a crystalline electric field and spin-orbit coupling. Comparison of the model predictions, including the effects of the impurity-electron–conduction-electron mixing interaction in a perturbation treatment, with data on magnetic susceptibilities and on magnetic atom hyperfine fields, leads to the conclusions that (a) Cr and Mn have the structure which corresponds to the free ion divalent configuration while Fe corresponds to a monovalent configuration, (b) the crystal field at the site of the magnetic atoms is opposite of that usually assumed, and (c) the Weiss temperature of *Cu*Cr is 2.9 ± 1.0 K.

I. INTRODUCTION

Iron group atoms in insulators are now well understood. The same is not true when the host is a metal. The experimental methods which have been so important for insulating hosts do not reveal enough information (ESR) or do not work [electron-nuclear double resonance (ENDOR)] in metallic hosts. We have studied the NMR of Cu atoms which are near neighbors to Cr atoms in dilute alloys of Cr in Cu. We find that the NMR frequencies of these atoms have an anomalous temperature dependence compared with those found for Cr atoms which are near neighbors to Mn or Fe atoms in similar dilute alloys, but can explain the data by an analysis which leads to a detailed picture of the electronic structure of these and other iron group atoms in Cu.

The understanding of dilute alloys of magnetic impurities in nonmagnetic metal host is far from complete. The term "magnetic" itself needs further clarification when applied to a magnetic impurity which is placed in a nonmagnetic metal. The mixing interaction between the impurity electrons and conduction electrons tends to reduce the magnetic nature of the impurity atom. If the mixing interaction is strong enough, the magnetic susceptibility of the atom in a metal is nearly independent of temperature, and much smaller than is typical for that species in an insulator. We then say the atom is "nonmagnetic" in the metal. If the mixing interaction is weak enough, the susceptibility obeys a Curie-Weiss law, and at temperatures comparable to or larger than the Weiss temperature T_K the magnetic susceptibility is comparable to values found for the atomic species when imbedded in insulators. We then say the atom remains "magnetic" in the metal. Cr, Mn, and Fe in Cu are examples of the latter behavior.

The absence of detailed experimental knowledge of the magnetic atoms in nonmagnetic metals has permitted a variety of theoretical descriptions, differing principally in the nature of the assumptions about the magnetic atom and its interaction with the electrons of the host-metal conduction band. Historically three models have been of particular importance: (1) the so-called "*s-d*" model, (2) the Friedel-Anderson model, and (3) the Hirst model which is closely related to a picture proposed by Schrieffer and Mattis. All three models may be described in terms of the general Hamiltonian:

$$H = H_e + H_{\text{imp}} + H_{\text{mix}} \ , \tag{1}$$

where H_e describes the conduction electrons, H_{imp} describes the impurity, and H_{mix} describes the mixing between the conduction electrons and the impurity electrons. For the iron group impurities, to which we are restricting this discussion, the important mixing is that between the impurity *d* electrons and components of the conduction electron wave functions which may be expressed as *d* components. H_e represents the kinetic and potential energy of the conduction electrons; since it is the same for all three models, we do not discuss it in further detail at present.

We have conducted experiments on the *Cu*Cr system using the technique of satellite NMR (which is reviewed later in this article). To our surprise, the temperature dependence of the results possessed

most unusual properties. In attempting to explain them we have found that the results shed a good deal of light on the electronic structure of the iron group impurities. We find that one of the above theoretical pictures gives a simple, natural explanation of the results. In Sec. II we review in more detail the theoretical and experimental background. At the end of Sec. II we give an outline of the rest of the paper.

II. BACKGROUND

A. Theoretical background

The earliest attempts[1] to treat the magnetic impurity problem used the *s-d* model which assumes that the impurity has net spin $\vec{S}$ and magnetic moment $g\mu_B\vec{S}$, where μ_B is the Bohr magneton and g is a constant of proportionality called the "g value." This model makes no attempt to deduce the spin and g value from first principles. The magnetic susceptibility of such an atom would obey Curie's law were it not for the mixing with the conduction electrons. The form of mixing interaction assumed is an exchange interaction:

$$H_{\text{mix}} = -J \sum_i \vec{S}\cdot\vec{s}_i\delta(\vec{r}_i) \tag{2}$$

with the ith electron of spin $\vec{s}_i$. This model leads to the Kondo effect,[2,3] and thus explains why the magnetic susceptibility obeys a Curie-Weiss law rather than Curie's law.

Friedel[4] viewed the problem as a scattering problem, distinguishing magnetic from nonmagnetic atoms by whether or not the up-spin and down-spin scattering resonances were at different energies (magnetic atom) or coincident in energy (nonmagnetic atom).

Anderson[5] proposed a modification of the Friedel approach to explain why some atoms were magnetic, whereas others were not. (In essence, circumstances which lead to an energy splitting between the up and down spin resonances.) In its simplest form, his theory takes the impurity orbital state to be nondegenerate and approximates

$$H_{\text{imp}} = E(n_\uparrow + n_\downarrow) + U(n_\uparrow n_\downarrow) \ , \tag{3}$$

where the number operators refer to the d electrons on the impurity. The term proportional to E represents the binding energy of the Coulomb potential. The term proportional to U represents the Coulomb repulsion between opposite spin states due to the symmetric spatial part of their total two-electron wave function. Anderson uses a mixing term of the form

$$H_{\text{mix}} = \sum_{k,\sigma} V_{dk}(c^\dagger_{k\sigma}c_{d\sigma} + c^\dagger_{d\sigma}c_{k\sigma}) \ , \tag{4}$$

where the $c^\dagger_{k\sigma}$ operator creates a conduction electron with wave vector k and spin σ and $c^\dagger_{d\sigma}$ creates an impurity d electron with spin σ. The Coulomb term in H_{imp} tends to make the impurity magnetic while the mixing term tends to break down the magnetic moment. The relative size of these two interactions determines whether or not a moment exists. The form of the mixing [Eq. (4)] makes the Hamiltonian a many-body Hamiltonian; Anderson treated it in Hartree-Fock (HF) approximation. With the HF approximation, the Anderson model produces virtual bound states with a width Δ which is determined by the strength of the mixing interaction. The condition for the survival of a magnetic moment in the presence of the mixing interaction is then expressed in terms of the ratio U/Δ—if the ratio is large enough the moment survives. Blandin[6] expanded on Anderson's suggestions to treat the orbitally degenerate case. Coqblin and Blandin[7] have treated the orbitally degenerate Anderson Hamiltonian with a spin-orbit interaction added. Schrieffer and Wolff[8] showed that in the strongly magnetic limit the *s-d* form for the mixing interaction can be derived from the Anderson form.

Schrieffer and Mattis[9] argued that the Hartree-Fock approximation did not treat the correlation energy properly, unduly favoring magnetism. They emphasized the importance of orbital degeneracy and Hund's rule matrix elements in stabilizing the moment. Our results strongly support such a picture.

Anderson's model treats the Coulomb interaction as large and important. The fact that some $3d$ alloys do have a Curie-Weiss magnetic susceptibility and hence a magnetic moment indicates that, in terms of his model, U/Δ must be greater than unity for at least the magnetic alloys. Thus Anderson recognizes that H_{imp} is larger than H_{mix} for the magnetic alloys. Hirst[10] argues that if H_{imp} is larger than H_{mix} it should be treated in more detail than Anderson treats it before the mixing interaction is considered. Hirst models the magnetic impurity atom in a metal host in close analogy to its circumstances in an insulator. Flynn, Peters, and Wert[11] independently concluded that an ionic model was needed. They based their conclusions on extensive studies of the variation of the magnetic susceptibility of dilute liquid alloys of iron group atoms as the valence of the host alloy is changed.

Hirst's picture is closely related to the Schrieffer-Mattis concepts. In an insulator the number of d electrons on the magnetic atom is integral, depending solely on the ionic state of the atom. The magnetic atom d electron spins are coupled together to form a total spin $\vec{S}$ and the orbital angular momenta are coupled together to form a total angular momentum $\vec{L}$. The magnetic atom has a rich atomic level structure including L-S, crystalline electric field, and spin-orbit splittings. Hirst argues that the atomic structure of

the magnetic atom is not much different when it is in a metallic host—the level splittings change somewhat, but the basic structure remains. The integral $3d^n$ electronic configurations will have different energies in general: designating the configuration with the lowest energy ground state as $3d^n$, the $3d^{n-1}$, and $3d^{n+1}$ configuration ground states have higher energies. The impurity electron-conduction electron interaction mixes the configurations to some extent, giving the $3d^{n-1}$ and $3d^{n+1}$ configurations a lifetime broadened level width, but the ground state cannot decay in an energy conserving process and has a narrow width produced only by virtual decay processes. If the ground-state level width is less than the splitting between the ground-state $3d^n$ configuration and the first excited alternate configuration ground state, the impurity is characterized to a great extent by the $3d^n$ configuration; further if the width is less than the intraconfigurational fine structure splittings, the details of the atomic structure manifest themselves and are not obscured, contrary to widely assumed treatments with the other models. Having first treated the impurity Hamiltonian in detail, Hirst treats the mixing interaction as a perturbation.

B. Experimental background

Just as the many-body nature of the mixing interaction has hindered understanding of the theoretical aspects of the dilute alloys, the difficulty of measurements has hindered the establishment of the experimental facts. Most of the dilute alloys are a problem metallurgically, i.e., few of the impurities make nice, random solutions with any appreciable concentration of the impurity. The impurity atoms have a strong tendency to form clusters. Clusters of impurities often have a Curie-Weiss susceptibility with a much lower Weiss temperature than isolated impurities, and hence at low temperatures the clusters dominate the bulk susceptibility. It is only with very dilute concentrations (as low as 5 ppm) of impurities and a careful study of the concentration dependence that one can be certain one is measuring the susceptibility of isolated impurities. Bulk techniques in general are at a disadvantage for application to nonrandom solutions because they only measure average properties. Quantitative determinations are difficult. Our group has developed satellite NMR as a technique for probing dilute alloys. It avoids the problems of bulk measurements.

The NMR frequency of a Cu nucleus which is near a magnetic impurity atom is shifted relative to that of pure Cu by a change in Knight shift. The shift of the Cu Knight shift, ΔK, from its value, K, in pure Cu produces weak resonances called "satellites" in the tails of the "main line" resonance produced by Cu nuclei more distant from all impurities. In samples of metal powder ΔK arises primarily from the isotropic hyperfine coupling and hence is due to the Fermi contact interaction. It thus represents a spin polarization of the conduction electrons.

During their study of *Cu*Cr near room temperature, Aton, Stakelon, and Slichter[12] found that the satellite resonances have an anomalous temperature dependence. We have followed the temperature variation of ΔK from 8.0 to 334 K for two neighbor shells and from 8.0 to 278 K for a third shell. For *Cu*Fe[13,14] and *Cu*Mn[15], $\Delta K/K$ obeys a Curie-Weiss law. The data from *Cu*Cr have a marked deviation from a Curie-Weiss law; however, all three satellites exhibit the *same* temperature dependence. In this article we provide detailed data and theory in support of an ionic model, only sketched in previous publications,[16,17] we have used to explain the observed temperature dependence. The basic concepts of the model follow Hirst; however we find it necessary to modify some aspects in order to account for the behavior of *Cu*Cr, *Cu*Mn, and *Cu*Fe. We demonstrate satisfactory agreement between the model and the data for all three of these alloys.

In Sec. III we develop the ionic model following Hirst. We discuss the treatment of the mixing interaction and the spin polarization which it produces in the conduction electrons. We describe the calculation of the spin and orbital magnetic susceptibilities, including the effects of the mixing interaction. Finally, we describe the calculation of the impurity hyperfine fields from the model.

In Sec. IV we discuss the experimental procedures using the gathering the NMR satellite data on *Cu*Cr.

In Sec. V we compare the experimental data with the model developed in Sec. III. We show that the *Cu*Cr NMR satellite data can be fitted by the model and determine the model parameter values. Comparison of the bulk impurity magnetic susceptibility of *Cu*Cr, calculated from the model with no additional free parameters, with the published data shows agreement within the experimental uncertainties. Extending the model comparison to *Cu*Mn and *Cu*Fe, we find good agreement with the available data.

In Sec. VI we discuss other related experiments.

Section VII is a summary and a discussion of possible future experimental and theoretical work which should yield further understanding of the dilute magnetic alloys.

III. THEORY

In order to understand how information about the magnetic impurity state can be deduced from NMR satellite data, it is necessary to understand the interactions which are included in the unperturbed impurity Hamiltonian H_{imp}, the effect of the mixing interaction H_{mix}, the relationship between the impurity magnetic susceptibility and the satellite data, and the

calculation of the susceptibility from the model. We also discuss the hyperfine fields predicted by this model.

A. Ionic impurity model

We follow Hirst[18] in development of the basic picture of the ionic impurity. The level splittings we consider, in order of decreasing size, are as follows:

(1) A balance between the Coulomb repulsion energy and the one-electron binding energy stabilizes a definite $3d^n$ configuration with splittings of about 10 eV.

(2) The Coulomb interaction splits the many-electron state into L-S terms with splittings of about 1 eV.

(3) A crystalline electric field splits the orbital states by about 0.1 eV.

(4) The spin-orbit coupling further splits the crystal-field-split orbital states by approximately 0.01 eV.

The orbital angular momenta of the impurity d electrons couple together to give a many-electron orbital angular momentum $\vec{L}$; similarly the spins couple to yield a many-electron spin $\vec{S}$. The Coulomb interaction splits the various L-S terms.

The energy of an electronic orbital state localized at an atomic site within a crystal depends on its orientation with respect to the crystal due to the crystalline electric field present at the atomic site. Yafet[19] discussed the nature of the crystal field present at the site of an impurity in a Cu host and showed that it is composed of two contributions of nearly the same magnitude with opposite signs. Thus for a dilute alloy the sign of the crystal field depends crucially on the relative magnitude of the two terms.

In cubic symmetry the crystal field splits the five d one-electron orbitals into a doublet level with e_g symmetry ($3z^2-r^2, x^2-y^2$) and a triplet level with t_{2g} symmetry (xy, xz, yz). Hirst examined experimental evidence to determine which term is lower, concluding that the triplet is lower than the doublet; we find that it is necessary to assume that the *doublet* is the lower level in order to explain our data. In cubic symmetry the crystal field is customarily represented by an equivalent spin operator[20]

$$H_{\mathrm{CEF}} = (\Delta/120)(0_4^0 + 50_4^4) \ , \tag{5}$$

where the subscript indicates the rank and the superscript indicates the component of the spherical tensor operators. Since both contributions to the crystal field are constrained by symmetry to be of the form of Eq. (5), we let Δ represent the sum of both terms; its sign is determined by the larger of the two opposing terms.

The spin-orbit interaction, conventionally expressed

$$H_{\mathrm{so}} = \lambda \vec{L} \cdot \vec{S} \ , \tag{6}$$

couples the orbital and spin degrees of freedom. λ is positive for $3d^n$ configurations with n less than five and negative for configurations with n greater than five.

TABLE I. $3d^n$ ground-state L-S configurations.

n	L	S
4	2	2
5	0	$\frac{5}{2}$
6	2	2
7	3	$\frac{3}{2}$

The nature of the level structure of the many-electron, impurity state depends on the relative magnitudes of the L-S splitting, crystal-field splitting, and spin-orbit splitting. The spin-orbit splitting is always smaller than the L-S splitting. The three general types of structure are designated "strong," "intermediate," and "weak crystal field" depending on the size of the crystal field relative to the L-S and spin-orbit splittings.

Hirst adopts the intermediate crystal field approach; we find this assumption to be consistent with our data. The many-electron, ground state, L-S term is determined by the Hund rules. Table I gives the ground state L-S terms of the $3d$ configurations of immediate interest. Figure 1 shows how the crystal

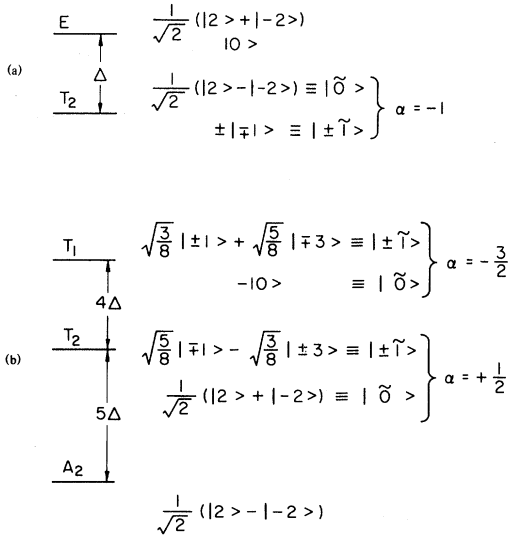

FIG. 1. (a) Cubic crystal-field splittings of a D ($L=2$) many-electron orbital state. The states given to the left are states of definite z component $\vec{L}$. The states with the tilde are fictitious angular momentum states with constant of proportionality α. The energy splitting is related to the crystal-field operator Eq. (5). (b) Cubic crystal-field splittings of an F ($L=3$) many-electron orbital state.

field represented by Eq. (5) splits the many-electron orbital states. The states given on the left in the figure are states of definite z component of $\vec{L}$. The states with the tilde are states of fictitious angular momenta. Matrix elements of $\vec{L}$ between these states are proportional to the matrix elements between the real states; the constant of proportionality is designated by α. These states are convenient for calculation of the magnetic susceptibility as described in more detail later in Sec. III D. For further details of the ionic structure see Ref. 20.

B. Mixing interaction

Schrieffer and Wolff[8] have shown that when the mixing interaction can be treated as a perturbation, the Anderson mixing interaction given in Eq. (4) taken to second order is equivalent to an interaction of the s-d form given by Eq. (2). Hirst[21] uses a mixing interaction of the form derived by Schrieffer and Wolff, but he allows for orbital degeneracy. He finds it convenient to use an irreducible-tensor operator notation for the purpose of calculations, but he gives a schematic form of the interaction projected onto the L-S ground state which makes the exchange form of the interaction more transparent (this form does not reveal the dependence on the wave vectors of the conduction electrons present in the tensor operator formalism)[18]:

$$H_{\rm mix}=J_S\vec{S}\cdot\vec{s}+J_L\vec{L}\cdot\vec{l}+J_{LS}\vec{L}\cdot\vec{l}\,\vec{S}\cdot\vec{s}+\cdots\ , \qquad (7)$$

where $\vec{L}$ and $\vec{S}$ refer to the orbital and spin angular momenta of the impurity and $\vec{l}$ and $\vec{s}$ refer to the orbital and spin angular momenta of the conduction electron. This form shows that the mixing interaction couples both the orbital and the spin angular momenta of the impurity to the conduction electrons.

We use Hirst's alternate form of coupling

$$H_{\rm mix}=\sum I_{kk'}a^{\dagger}_{m\sigma}a_{m'\sigma'}c^{\dagger}_{k'm'\sigma'}c_{km\sigma}\ ,$$

where the operator $a^{\dagger}_{m\sigma}$ creates an impurity electron with z component of orbital angular momentum m and of spin σ, and the operator $c^{\dagger}_{km\sigma}$ creates a conduction electron with wave vector magnitude k, z component of orbital angular momentum m and of spin σ. $I_{kk'}$ is a matrix element which depends on k and k'. The dependence of the mixing interaction on spatial distribution and wave vectors of the conduction electrons is contained in $I_{kk'}$.

C. Spin polarization

The mixing interaction causes some of the magnetic moment which is localized at the impurity site before the mixing perturbation is applied to "leak out" into the crystal in the neighborhood of the impurity, polarizing the conduction electron spins in an oscillating, damped, spin-density wave. Thus the spin density of the conduction electrons at the host crystal sites in the vicinity of the impurity is changed from the density which exists in the pure host metal. In a metal, the polarization of the conduction electrons at the nuclear sites couples to the nuclear moment by means of the hyperfine interaction to produce the Knight shift. Therefore, in the alloy, the spin-density wave changes the Knight shift of a host nucleus which is a near neighbor of the impurity from that of the pure host metal. The change ΔK from the pure host Knight shift K produces weak resonances called "satellites" in the tails of the "main line" resonance produced by host nuclei more distant from all impurities. In a powder each neighboring shell of nuclei will in general produce a distinct satellite. The size of ΔK for each shell, the width and intensity of the satellite resonances, and the quality of the measurement determine whether or not the satellites are resolved from the mainline and each other.

In Appendix A we show that

$$\frac{\Delta K}{K}=g(\vec{r})\chi^S(T)\ , \qquad (8)$$

where $\chi^S(T)$ is the magnetic spin susceptibility of the impurity and $g(\vec{r})$ gives the spatial dependence of the spin-density wave. The temperature dependence of the satellite splittings is thus entirely determined by the impurity spin susceptibility. Conversely, by determining the temperature dependence of the satellite splittings, we can determine the temperature dependence of the impurity spin susceptibility.

D. Impurity magnetic susceptibility

The ground state of the impurity has a magnetic susceptibility which consists of a temperature independent contribution, plus a temperature dependent contribution that obeys a Curie-Weiss law. The concept of a temperature independent *orbital* susceptibility is quite familiar. It arises from admixture of a higher energy orbital state into the ground state by the applied magnetic field and gives an orbital susceptibility of order

$$\chi^L\simeq\frac{\mu_B^2}{\Delta}\ , \qquad (9)$$

where μ_B is the Bohr magneton and Δ is the energy splitting to the excited orbital state.

A temperature independent spin susceptibility arises when the spin Zeeman coupling admixes higher states into the ground state. If one neglects spin-orbit coupling, the ground-state wave function is a product of an orbital wave function with a spin function of definite m_s. Then the ground state is already an eigenstate of S_z, so that there are no nonzero matrix elements of the spin Zeeman interaction between the ground and excited states. On the other hand, if

one includes spin-orbit coupling, it may happen that the states prior to application of the magnetic field consist of a sum of products of orbital functions with states of different values of m_s. Then the spin Zeeman interaction will tend to change the weighting of the various m_s components in order to best take advantage of the magnetic polarization thereby induced and one gets a temperature independent contribution to the spin susceptibility.

When the ground state has orbital and spin angular momenta, $\vec{L}$ and $\vec{S}$, coupled together to form a ground-state angular momentum, $\vec{J}$, S_z is not a good quantum number and the Zeeman interaction admixes excited states of the same $\vec{L}$ and $\vec{S}$ but different $\vec{J}$ into the ground state giving a temperature independent spin susceptibility of order

$$\chi^s \simeq \frac{\mu_B^2}{|\lambda|} \ , \tag{10}$$

where λ is the spin-orbit coupling parameter. If the ground-state orbital angular momentum is quenched but there is a spin-orbit multiplet of energy Δ higher due to the crystal field, one gets a temperature independent spin susceptibility of order

$$\chi^s \simeq -\frac{\mu_B^2 \lambda}{\Delta^2} \tag{11}$$

which should be smaller than Eq. (10) for reasonable crystal fields and is of the opposite sign for an atom with a positive spin-orbit coupling parameter.

In the detailed calculation of the susceptibility we first calculate the susceptibility of the impurity using the structure derived from H_{imp}. We then include the effect of H_{mix} as a perturbation. Since the highest temperature accessible experimentally is limited by the melting point of Cu to about 1300 K, and the crystal-field splittings are expected to be several thousand degrees, we have limited our calculation to population of the ground state of the crystal field only. Since spin-orbit splittings are on the order of 100 K we have allowed for the population of higher energy spin-orbit-split states in those cases where tne ground state of the crystal field has a first-order spin-orbit splitting.

E. Susceptibility without mixing

We need to consider four possible electronic configurations $(3d)^4$, $(3d)^5$, $(3d)^6$, and $(3d)^7$. The $3d^5$ configuration ground state has A_1 symmetry and no orbital angular momentum. The first excited state is split by the L-S splitting and probably lies on the order of 10 000 K above the ground state. We ignore all but the ground state. The susceptibility is then completely spin susceptibility with a moment corresponding to $S = 5/2$; there is no temperature independent contribution

$$\chi = \frac{g^2 \mu_B^2 S(S+1)}{3 k_B T} \ , \tag{12}$$

where g is the g value of the impurity d electrons.

If the crystal field causes the states with symmetry T_2 of the orbital D state [for example with $(3d)^4$ or $(3d)^6$] or the states with symmetry T_1 of an orbital F state [for example with $(3d)^7$] to be the ground state (see Fig. 1), we consider the ground state of the crystal field only. We write the spin-orbit Hamiltonian

$$H_{so} = \alpha \lambda \vec{L}_e \cdot \vec{S} \ , \tag{13}$$

relating the effective (fictitious) angular momentum operator $\vec{L}_e$ to $\vec{L}$ with constant of proportionality α. For the threefold degenerate state T_2, for example, $L_e = 1$ and $\alpha = -1$. The spin-orbit interaction couples $\vec{L}_e$ and $\vec{S}$ together to give states of total fictitious angular momentum F and z-component M_F. It lifts the $(2L_e+1)(2S+1)$ degeneracy of the ground state to give energies

$$\begin{aligned} E_F &= \frac{\alpha\lambda}{2}[F(F+1) - L_e(L_e+1) - S(S+1)] \ , \\ |FM_F\rangle &= \sum_{mm'} |LmSm'\rangle \langle LmSm'|FM_F\rangle \ , \end{aligned} \tag{14}$$

where the coefficients of the states in the sum are the Clebsch-Gordan coefficients. Having treated the spin-orbit interaction exactly (within the orbital ground state), we treat the Zeeman interaction as a perturbation which mixes the states given in Eq. (14). We calculate the expectation of L_z and S_z for each of these mixed states and compute the thermal averages, $\langle L_z \rangle$ and $\langle S_z \rangle$, in the usual way. The susceptibility is then derived from

$$\chi = -\frac{\mu_B N}{H}(\alpha k \langle L_{ez} \rangle + 2\langle S_z \rangle) \ , \tag{15}$$

where k is the orbital reduction factor which represents a reduction of the orbital angular momentum from that of a free ion due to the crystal environment (see Ref. 20). Both the spin and orbital susceptibilities have a temperature dependent contribution and a temperature independent contribution of the form of Eq. (10).

If the crystal field causes the state with symmetry A_1 of an orbital F state or the states with symmetry E of an orbital D state to be the ground states, the orbital angular momentum is quenched in the ground state and no first-order spin-orbit splitting exists. In this case we treat both the spin-orbit interaction and the Zeeman interaction as perturbations to the crystal-field interaction. The first-order perturbation correction to the ground state yields a temperature independent contribution to the orbital susceptibility of the form of Eq. (9) but no contribution to the spin susceptibility. The second-order perturbation correc-

tion to the wave function yields temperature independent contributions to both the spin and orbital susceptibilities of the form of Eq. (11) and a temperature dependent contribution to the orbital susceptibility.

For details on the calculation of the susceptibility for specific configurations see Appendix B.

F. Effect of mixing on the susceptibility

There are two effects of the mixing for which we must account quantitatively in order to obtain reasonable agreement between the calculated susceptibility and experiment: (1) the mixing produces an antiferromagnetic polarization of the conduction electrons and thus reduces the total experimentally measured susceptibility from that calculated in the previous section. This effect is most simply illustrated for Mn which is generally agreed to be in a ^6S, $(3d)^5$ state, with negligibly low Kondo temperature. (2) The Kondo effect causes the temperature dependence of the susceptibility to deviate from a Curie law.[22] We treat the antiferromagnetic coupling to the conduction electrons in perturbation theory as a reduction of the effective impurity moment. We treat the Kondo effect by replacing the temperature T with $T+\theta$ everywhere it appears in the expressions for the susceptibility.[22]

The experimental susceptibility of a dilute alloy is measured as the difference between the susceptibility of the alloy and that of the pure host metal; thus the experimental susceptibility includes not only the susceptibility of the impurity moment calculated as described in the previous section, but also the susceptibility of the induced conduction electron polarization. At temperatures far above the Kondo temperature the mixing interaction can be treated as a perturbation.

If the ground-state angular momentum is quenched by the crystal field, only the first term in Eq. (7) produces a polarization of the conduction electrons $\langle s_z\rangle$ and we find

$$\langle s_z\rangle = \langle s_z\rangle_0 - J_s\rho\langle S_z\rangle \ , \tag{16}$$

where ρ is the density of states at the Fermi surface for one spin direction, and $\langle s_z\rangle_0$ is the polarization of the conduction electrons which would exist in the absence of the impurity (see Ref. 24). The total experimentally measured susceptibility thus takes the form

$$\chi_{\text{expt}} = (1-J_s\rho)\chi^S + \chi^L \ , \tag{17}$$

where χ^S and χ^L represent the spin and orbital susceptibilities of the impurity, respectively. It is customary to define an effective magnetic moment such that

$$\chi^S = \frac{\mu_{\text{eff}}^2}{3k_BT} \ . \tag{18}$$

We write

$$\chi_{\text{expt}} = \eta^2\chi^S + \chi^L \tag{19}$$

such that $\eta^2 = 1 - J_S\rho$ and η thus represents the reduction in the effective magnetic moment due to the conduction electron polarization.

If the ground-state orbital angular momentum is not quenched, the form of the mixing interaction is quite complicated. To our knowledge the form of polarization induced by the general form of the mixing interaction has not been calculated. The experimental precision with which the magnetic moments of the impurities have been measured to date does not require great accuracy; therefore we make the assumption that the spin and orbital susceptibilities are affected equally because of the spin-orbit coupling and use

$$\chi_{\text{expt}} = \eta^2\chi_{\text{imp}} \tag{20}$$

with

$$\eta^2 = 1 + J\rho \ , \tag{21}$$

where J is now a parameter which defines the strength of the interaction. We let $J_s = -J$ in the case described by Eq. (19); then Eq. (21) suffices to describe the reduction of the magnetic moment for all cases.

Near the Kondo temperature higher order perturbation terms in the mixing become important, and in fact as the temperature approaches the Kondo temperature the coupling becomes so strong as to make perturbation theory invalid—a calculation such as a renormalization-group theory calculation is required. Krishna-murthy, Wilson, and Wilkins[3,22] have done such a calculation using both the s-d [Eq. (2)] and Anderson [Eq. (4)] forms of the mixing interaction for a spin-$\frac{1}{2}$ impurity. They find that, indeed, the two forms of interaction yield results in the experimentally accessible temperature regime identical to those predicted by Schrieffer and Wolff.[6] At temperatures above the Kondo temperature, they find the susceptibility can be described over any decade of temperature by a Curie-Weiss law with a moment decreased from the Curie moment. Below the Kondo temperature the susceptibility becomes constant. Although the calculation is for a spin-$\frac{1}{2}$ impurity, it explains the temperature dependence of the susceptibility of *Cu*Fe and *Cu*Mn over the entire temperature range for which it has been experimentally determined. It does *not* explain the temperature dependence of the susceptibility of *Cu*Cr.

We take the failure of the renormalization-group calculation which included no orbital degrees of freedom, to explain the temperature dependence of the susceptibility of *Cu*Cr to be further evidence that a model with orbital structure is necessary to describe the magnetic impurities. Unfortunately, to our

knowledge no calculation of even the perturbation type, other than that which we give in Appendix A, has been done with the more complete form of mixing interaction [Eq. (7)]. Following the results of the spin-only renormalization-group calculation, we compute the susceptibility by reducing the effective moment according to Eq. (21) and replacing T everywhere it occurs in the expression for the susceptibility with $T+\theta$. This expression yields the Curie-Weiss law behavior when only the ground state of the spin-orbit splitting is populated and passes smoothly into the proper high-temperature form. We have not attempted to deduce the behavior at temperatures below the Kondo temperature.

It remains to determine the value of J to be used in calculating the reduction of the moment [Eq. (21)]. For the spin-only case Wilson[22] gives an expression which relates the exchange coupling constant for the spin-only interaction j to the Kondo temperature

$$T_K = D(\rho|j)^{1/2}\exp(-1/\rho|j|) \ . \tag{22}$$

In the spin-$\frac{1}{2}$ case, at temperatures just above the Kondo temperature θ Weiss temperature in the Curie-Weiss susceptibility, is $2T_K$.[3] From the observed Curie-Weiss temperature dependence we determine T_K and then use Eq. (22) to find j. J is roughly j times the number of orbital degrees of freedom available for the mixing interaction; thus for a completely symmetric A_1 ground state with the full orbital degeneracy of the $L=2$ state, $J=5j$.[6] Hirst[23] has calculated the reduction in the effective degrees of freedom which a crystal field produces. He expresses this reduction in terms of the ratio of the first order Born approximation to the resistivity ρ_{1B} to the second-order Born approximation term which produces the Kondo effect ρ_{2BK}. For a crystal-field-split ground state we have

$$J = 5j\left(\frac{\rho_{1B}}{\rho_{2BK}}\right)_{L-S}\left(\frac{\rho_{2BK}}{\rho_{1B}}\right)_{\mathrm{CEF}} \ , \tag{23}$$

where the subscript CEF refers to the resistivity which obtains when a crystal field is present and L-S refers to the resistivity which would exist if there were no crystal-field splitting. In cases where the crystal-field ground state is split by a spin-orbit coupling which is much larger than the Kondo temperature, we further reduce the expression given by Eq. (23) by the ratio of the degeneracy of the crystal-field ground state

$$J = 5j\left(\frac{\rho_{1B}}{\rho_{2BK}}\right)_{L-S}\left(\frac{\rho_{2BK}}{\rho_{1B}}\right)\frac{2F+1}{3(2S+1)} \ . \tag{24}$$

G. Hyperfine fields

The hyperfine interaction between the impurity nucleus and the impurity electronic state may be expressed

$$H_{\mathrm{hf}} = g_N\mu_N\vec{\mathrm{I}}\cdot[H_L\vec{\mathrm{L}}+2(H_S)\vec{\mathrm{S}}] \ , \tag{25}$$

where the subscript N denotes the nucleus and where Eq. (25) defines the so-called orbital and spin saturation magnetic and fields H_L and H_S, respectively. Narath[24] has calculated the values of the saturation hyperfine fields expected for $3d$ transition metals with a Hartree-Fock approximation. For *Cu*Fe enough experimental evidence exists to determine the saturation hyperfine fields from our model and compare these values with those of Narath's calculation. If the ground state of the impurity has zero angular momentum, the orbital hyperfine contribution vanishes (except to the extent that the Zeeman interaction causes mixing with excited states with unquenched orbital angular momentum) giving a total hyperfine saturation field:

$$H_{\mathrm{hf}}^{\mathrm{sat}} = 2SH_S \ . \tag{26}$$

For cases in which the ground-state orbital angular momentum is not quenched, we project the hyperfine interaction onto the spin-orbit ground state

$$H_{\mathrm{hf}}^{\mathrm{sat}} = -2(S_z)H_S - k\alpha(L_{ez})H_L \ , \tag{27}$$

where (S_z) and (L_{ez}) are the effective saturated z components of the spin and fictitious angular momentum of the spin-orbit ground state. Details for specific impurities are given in Sec. V.

IV. EXPERIMENTAL PROCEDURES

The *Cu*Cr powders used in this experiment were prepared by Boyce and Stakelon as part of a general alloy preparation program which produced dilute alloys of all of the $3d$ transition metals in copper. Details of the sample preparation procedure are given by Boyce.[25] The samples were prepared from 99.999+% pure Cu rod (American Smelting and Refining Company) and 99.999% pure Cr lumps (United Mineral and Chemical Corporation). The Cu and Cr were heavily etched to remove surface contaminants. The appropriate proportions of Cu and Cr were placed in alumina crucibles inside quartz tubes and baked in vacuum to remove water vapor. The quartz tubes were then back filled with $\frac{1}{4}$ atmosphere of pure argon and sealed. After baking for 1 h in an induction furnace at 1200 °C, the tubes were rapidly quenched to 20 °C in water. The alloys were then wrapped in 5-mil copper (99.9% pure) foil and swaged to less than half of their original diameter to improve homogeneity. The copper foil was removed and the surface etched away. The alloys were again sealed with argon in quartz tubes, annealed for approximately 3 d at 30 to 70 °C below the melting point, and then quenched in water. The surface was again etched and

the alloy rod was ground to powder with a rotary grinder with a tungsten carbide cutter. For maximum penetration by the rf field, only powder which passed through a 400 mesh (less than 37 μm) sieve was used. None of the powders were reannealed.

Analyses of the annealed rods were made from pieces cut from both ends prior to grinding. The Cr concentrations were homogeneous to about 5%. The analyses yielded average Cr concentrations of 0.56, 0.102, 0.051, and 0.017 at.% for alloys which were nominally 0.5, 0.1, 0.05, and 0.01 at.%, respectively. The 0.56 at.% alloy was examined under a microscope for macroscopic inhomogeneities. Electron microprobe analysis also showed the alloys to be homogeneous to about 5%.

For historical reasons three spectrometers were used in this study. The first data obtained were taken by Aton at temperatures of 230 K and higher in a high field spectrometer with a room temperature access dewar. When he noticed an anomalous temperature dependence to the satellites, we continued the study in a low-field spectrometer with a double glass dewar. With this spectrometer we were able to make measurements at liquid-nitrogen (77 K), liquid-neon (27 K), and liquid-helium (4.2 K) temperatures. When we failed to observe the satellites at 4.2 K, it became necessary to use a cryostat which allowed operation at temperatures between 27 and 4.2 K. The high field solenoid used for the high-temperature measurements also has a cryostat dewar which allows temperature control over this temperature range; thus we inserted the cryostat into the high field solenoid and assembled a spectrometer compatible with the cryostat. All three spectrometers are hybrid-junction, bridge spectrometers.

Temperature control in a magnetic resonance experiment at temperatures of a few degrees kelvin causes a problem. Ideally one would like to have the sample, thermometer, heating element, and controller temperature sensor all in excellent thermal contact. To prevent stray rf pickup the heating element with its relatively large currents must be kept electrically isolated from the rf coil. These two constraints require that the material separating the sample and the heating element be a poor electrical conductor but a good thermal conductor at these temperatures. For handling, the material must be rigid at room temperature. The only material of which we are aware that meets these criteria is solid sapphire. Besides being expensive, sapphire has an ^{27}Al NMR which would swamp the weak satellite signals.

We have adopted a compromise approach to the temperature control problem. The temperature of a large thermal mass (the brass can and lid and the copper foot) which surrounds the sample is controlled. Good thermal contact is established between the thermal mass, heating element, and controller temperature sensor, but a temperature gradient is allowed to develop between the thermal mass and the sample. A thermometer which requires only a small dc current and is protected from stray rf is placed in thermal contact with the sample. With the thermal mass, heating element, and controller temperature sensor in good thermal contact the temperature of the thermal mass can be controlled very stably. The poor thermal contact between the thermal mass and the sample means that it may take the system a while to come to equilibrium, but once equilibrium is reached the temperature of the sample should be nearly as stable as that of the thermal mass. The sample temperature can be read accurately with the thermometer because they are in good thermal contact.

With the help of P. Anthony we calibrated a GaAs diode (Scientific Instruments Model GA-300, SN 90251) from 4.210 to 96.4 K. The calibration was done in A. C. Anderson's cryostat using his Ge resistor thermometer (4182-R) as a secondary standard. The diode was calibrated with a four lead configuration and the voltages were read on a 10^{10}-Ω imput impedance digital voltmeter (DVM) which was first checked for calibration against a standard cell. A homebuilt constant current source consisting of a 741 operational amplifier with a memory reference cell provides 10 μA to a diode. Thermal cycling to room temperature and back down to 10 K revealed that the diode maintained its calibration to within the accuracy with which the voltage was read. The temperature was easily read to an accuracy of better than 0.1 K. A slight sensitivity to magnetic fields (an error of +0.1 K at 10 kOe followed by a drop to an error of −0.9 K at 55 kOe) was measured at 4.2 K and corrected for.

Four different impurity concentrations were used to verify the concentration independence of the satellite splittings and to optimize the experimental resolution of the satellites over the wide temperature range. At low temperatures the satellites become broader and more difficult to resolve; it is often easier to resolve the satellites in more dilute samples. The fields used in the experiment ranged from 5 to 55 kOe. At high temperatures a large field is necessary to split the satellites enough to resolve them; at low temperatures the splittings are larger and a lower field is advantageous. It is also important at low temperatures to use a field small enough to avoid saturation of the impurity moment, i.e., we want to measure the susceptibility in a field small enough that the susceptibility is essentially field independent. Table II shows the samples and field strengths used at the various temperatures at which data were taken. No concentration or field dependence was observed.

Cu has two isotopes with magnetic moments—^{63}Cu and ^{65}Cu. We verified that the satellite resonances are present for both Cu isotopes, thus confirming that the resonance we attribute to Cu nuclei which

TABLE II. Impurity concentrations and field strengths. The field strengths used at each temperature are given. The samples investigated are indicated by an *x*.

T (K)	Concentration (at.%) 0.56	0.102	0.051	0.017	Field (kOe)
334		x			
278	x	x			55
230		x			
77		x	x		10 to 23
27.1			x		10
15.1			x	x	12
8.0			x		
4.2			x	x	
3.0			x		5 to 12
2.5			x		
1.4			x		

are neighbors of the Cr impurity are indeed Cu resonances and not the spurious resonances of some other nuclei.

V. EXPERIMENTAL RESULTS

A. *Cu*Mn

*Cu*Mn is the simplest system. Since its configuration is $3d^5\ {}^6S$, it has no orbital effects. Its Kondo temperature is so low that the Kondo effect can be neglected at temperatures of 1 K or higher. It therefore illustrates clearly solely the effect of the mixing interaction in reducing the effective magnetic moment. The magnetic susceptibility is spin only and of the form of Eq. (12) with $S=5/2$ giving a "bare ion" magnetic moment of $5.92\mu_B$ compared with the experimental moment determined from measurements from room temperature down to a few degrees kelvin of $(4.9\pm0.3)\mu_B$.[26] Following the procedure outlined in Sec. III F, we find the effective moment to be $4.8\mu_B$. Aton's[15] NMR satellite data show a Weiss temperature of zero—consistent within the experimental uncertainty with the value of (9.5 ± 1.5) mK determined from the low-temperature bulk susceptibility measurements of Hirschkoff, Symko, and Wheatly.[27] Neither the NMR satellite data nor the bulk measurements show any temperature independent contribution to the susceptibility.

From Eq. (26) with the assumption that $S=5/2$ we have a saturation hyperfine field, $H_{\rm hf}^{\rm sat}=5H_S$. Davidov *et al.*[28] measured the value of $H_{\rm hf}^{\rm sat}$ to be -280 kOe—giving $H_S=-56$ kOe. Narath[24] gives a theoretical estimate of -25 kOe $\geq H_S \geq -140$ kOe. (We deduce a value of H_S for *Cu*Fe of -50 kOe in a later section.) Therefore, the Mn data can be explained readily in the Hirst picture.

B. *Cu*Cr

1. *NMR satellite data*

The NMR satellite data obtained in this investigation are displayed in Fig. 2. Since $\Delta K/K$ is proportional to the impurity spin susceptibility [see Eq. (8)], we have plotted $K/\Delta K$ versus the temperature; on such a plot a Curie-Weiss law appears as a straight line which intercepts the abscissa at the negative of the Weiss temperature. The dashed lines are straight lines drawn through the low-temperature data; the uncertainties of the low-temperature data are sufficiently small to require the slopes shown. The data deviate by about 20% from the Curie-Weiss law at 300 K. It is fortunate that the satellite labeled "C" is shifted to the opposite side of the main line from N and P. Because all three satellites are shifted closer to the abscissa (further from the main line) than the Curie-Weiss law predicts, we know that the deviation is not due to a shift in the main line resonance caused by some experimental error.

We compare the data with the model developed in Sec. III which first treats the impurity structure in detail and then treats the mixing interaction as a perturbation. Following Hirst we first attempt a fit to the $3d^4$, E symmetry ground state which results if the t_{2g} symmetry single-electron orbitals have lower energy than those with e_g symmetry. Starting from the results in Appendix B we calculate for the spin susceptibility

$$\chi^S=8\mu_B^2N\left(\frac{1}{k_BT}-\frac{2\lambda k}{\Delta^2}\right)\ . \tag{28}$$

A Cr^{2+} ion ($3d^4$) has a spin-orbit coupling λ of $+58$ cm^{-1},[20] and therefore the temperature independent

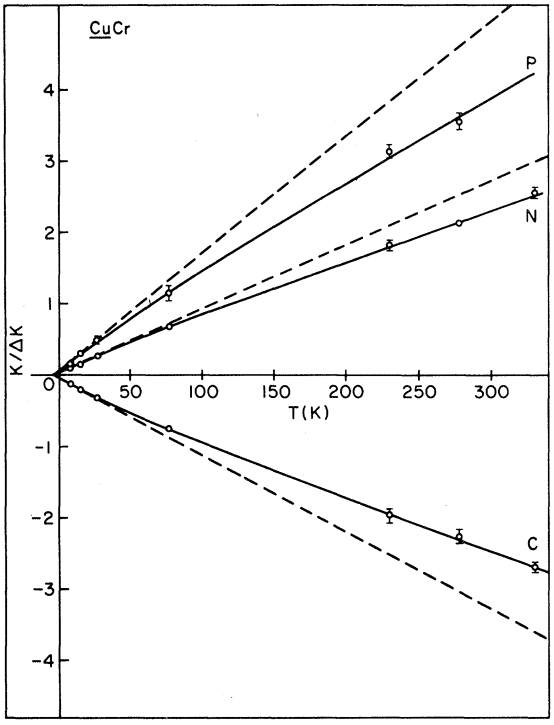

FIG. 2. A plot of the *Cu*Cr satellite data. The dashed lines represent a Curie-Weiss law fit to the low-temperature data. The solid lines are the fit to the model described in the text.

term in Eq. (28) is negative while the fit to the satellite data indicates a positive temperature independent term; thus Hirst's assignment of the ground state does not explain the satellite data.

Comparison of the experimental evidence on *Cu*Cr and *Cu*Fe gives a clue as to what is happening. Both *Cu*Cr[29,30] and *Cu*Fe[31] have a temperature independent contribution to their bulk magnetic susceptibility; but although the *Cu*Cr satellite data show a 20% temperature independent contribution to $\Delta K/K$ at 300 K, no temperature independent contribution to the satellite data is observed for *Cu*Fe to within the experimental uncertainties (see, however, discussion under Sec. VI D).[13] The indication is that the ground state of Cr has an unquenched orbital angular momentum with a temperature independent contribution to the spin susceptibility of the form of Eq. (10) while the ground state of Fe has its orbital angular momentum quenched and a temperature independent contribution to its spin susceptibility like Eq. (11) which is expected to be smaller than that of Eq. (10). If the t_{2g} symmetry single-electron orbitals are lower than those with e_g symmetry as Hirst suggests, the $3d^4$ configuration has an E symmetry ground state with quenched orbital angular momentum and the $3d^6(Fe^{2+})$ and $3d^7(Fe^{+})$ configurations have T_2 and T_1 symmetries, respectively, with unquenched orbital angular momentum. This assignment disagrees with the conclusion made from the bulk susceptibility and satellite data. If the sign of the crystal field is opposite of that assumed by Hirst so that the e_g symmetry single-electron orbitals have lower energy than those with t_{2g} symmetry, the $3d^4$ configuration ground state has T_2 symmetry with unquenched orbital angular momentum and the $3d^6$ and $3d^7$ configurations have E and A_2 symmetries, respectively, with quenched orbital angular momentum; thus by assuming the sign of the crystal field opposite of that usually proposed, we can qualitatively account for the experimental evidence on *Cu*Cr and *Cu*Fe. In the following discussion we attempt to make the agreement quantitative.

If the crystal field causes the e_g single-electron orbitals to have lower energy than the t_{2g} symmetry orbitals, the $3d$ atomic level structure is that shown in Fig. 1(a). The ground state has T_2 symmetry with fictitious angular momentum $L_e = 1$. The spin-orbit interaction couples the orbital and spin states ($S = 2$) to give states of total fictitious angular momentum F. The resultant level structure is shown in Fig. 3. Note that only first-order spin-orbit splittings are shown. Higher order spin-orbit terms split the remaining degeneracies down to the degeneracies required by symmetry. These higher order splittings, except those in the $F = 3$ ground state where the splittings can become of the order of the temperature or greater, are unimportant for calculation of the susceptibility. We ignore the higher order splittings for the moment and will discuss them further when we discuss the low-temperature bulk susceptibility data.

As discussed in Sec. III B, the crystal-field splitting is expected to be several thousand degrees; we ignore

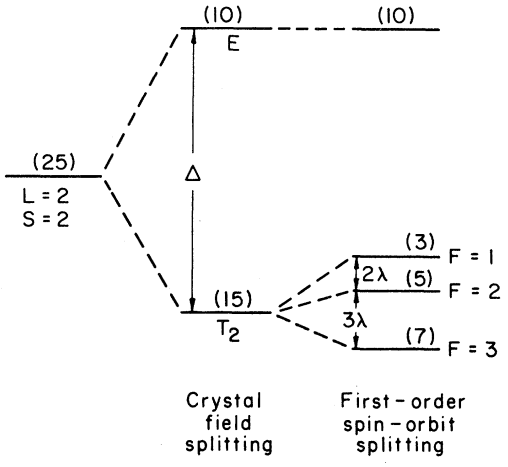

FIG. 3. The level structure of Cr^{2+} showing the effect of the crystal field and first-order spin-orbit coupling. The numbers in parentheses indicate the degeneracies of the levels.

TABLE III. Fit of model to *Cu*Cr NMR satellite data. The NMR data are compared with the model calculation for satellites *N*, *P*, and *C*. The experimental uncertainties are given in parentheses.

T (K)	$(\Delta K/K)_N$ expt	$(\Delta K/K)_N$ calc	$(\Delta K/K)_P$ expt	$(\Delta K/K)_P$ calc	$(\Delta K/K)_C$ expt	$(\Delta K/K)_C$ calc
334	0.39 (1)	0.396			−0.37 (1)	−0.363
278	0.469 (7)	0.469	0.281 (9)	0.276	−0.44 (2)	−0.430
230	0.55 (2)	0.558	0.32 (1)	0.328	−0.51 (2)	−0.511
77	1.48 (6)	1.45	0.87 (8)	0.851	−1.31 (6)	−1.33
27.1	3.58 (8)	3.54	2.0 (2)	2.08	−3.2 (1)	−3.24
15.1	6.1 (4)	5.76	3.1 (4)	3.38	−5.0 (3)	−5.27
8.0	9.1 (6)	9.38	5.8 (3)	5.51	−8.5 (5)	−8.59

the excited crystal-field-split E symmetry states. Since the spin-orbit coupling parameter in Cr^{2+} is 84 K, we include all of the spin-orbit-split T_2 states. Each spin-orbit-split level has a Curie-Weiss law contribution to the susceptibility plus a temperature independent contribution that results from mixing of the spin-orbit-split states by the Zeeman interaction. Thus the susceptibility of the Cr arises primarily from the $F=3$ ground state with some contribution from the excited $F=2$ and $F=1$ states at the higher temperatures. A computer fit to the satellite data, allowing the Weiss temperature, spin-orbit coupling parameter, and the orbital reduction factor to be free parameters, yields the fit shown in Fig. 2 and tabulated in Table III with $\theta=2.9\pm1.0$ K, $\lambda=48\pm32$ cm^{-1}, and $k=0.84\pm0.19$. The normalized χ^2 of this fit to the data is 0.56. The orbital angular momentum and spin-orbit coupling are both reduced to about 80% of the free ion values. Such a reduction is to be expected and is of a reasonable magnitude.[20] The large uncertainty in the determination of the parameters is due to the strong interdependence of the parameters. The uncertainties quoted are the amount of change necessary in a given parameter to change the normalized χ^2 of the computed fit by one.

The fit shown in Fig. 2 and tabulated in Table III, based on the assumption that the satellite splittings are proportional to the impurity spin susceptibility only, appears to explain the data quite well. We also tested the hypothesis that the splittings are proportional to the *total* impurity susceptibility. The fit thus obtained is not as good as the fit to the spin susceptibility only; furthermore the value of the spin-orbit parameter required to produce the fit is 350 ± 160 cm^{-1} and the magnetic moment obtained from the fit is $3.2\mu_B$. The experimental value for the moment is $(3.7\pm0.4)\mu_B$ (see the following section). The Cr^{2+} free ion has a spin-orbit coupling parameter of 59 cm^{-1}. The spin-orbit interaction is expected to be reduced slightly in the metal host—certainly not increased by a factor of 6. We conclude that the fit to the total susceptibility is unphysical while the fit to the spin susceptibility gives empirical evidence that the satellite splittings are proportional to the spin susceptibility only and thus Eq. (8) is correct.

2. *Bulk magnetic susceptibility data*

Due to the spin-orbit coupling the spin and orbital susceptibilities are not independent; the determination of the model parameters from the satellite data allows calculation of the bulk susceptibility. The only additional factor required is η^2, the mixing reduction parameter, which is calculated from Eq. (24). The calculated susceptibility is plotted versus $1/(T+2.9)$ in Fig. 4. Note that since the first excited spin-orbit-split state lies approximately 200 K above the ground state, the susceptibility becomes essentially a Curie-Weiss law plus a temperature independent term below about 100 K. Since the spin-orbit splittings become unimportant at temperatures much greater than

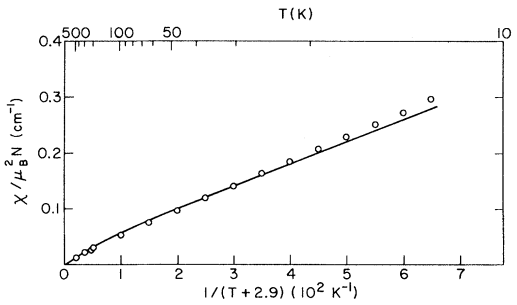

FIG. 4. The bulk magnetic susceptibility of *Cu*Cr. The curve is the susceptibility calculated from the model described in the text. The open circles are a representation of the experimental data of Hoeve and Van Ostenburg, and Vochten, Labro, and Vynckier as described in the text.

the total spin-orbit splitting (the sum of the temperature independent terms of the three spin-orbit split levels is zero), the temperature independent term vanishes and the susceptibility approaches zero at infinite temperatures. The Weiss temperature is assumed to be the same as that determined from the satellite data since the spin and orbit are coupled; the total effective magnetic moment in the low-temperature regime is calculated to be $(3.4 \pm 0.4)\ \mu_B$.

Vochten, Labro, and Vynckier[29] have reported a bulk susceptibility study of *Cu*Cr on three samples with 5-, 15-, and 112-ppm atomic concentrations of Cr at temperatures from 1.5 to 300 K and fields from 3.96 to 12.64 kOe. The susceptibility of the 5-ppm Cr samples was plotted versus the susceptibility of the 15-ppm Cr sample for all temperatures and fields. The fact that all the data fall on a straight line is strong evidence that the susceptibility measured is the susceptibility of isolated impurities only. A similar plot for the 112-ppm Cr sample versus the 15-ppm sample shows some deviation from a straight line for the low-temperature data; this deviation is attributed to cluster effects in the 112-ppm Cr sample. Vochten *et al.* use the ratio of the susceptibilities measured in the two most dilute samples to that measured in the 112-ppm sample to establish "more precise concentrations" for those samples—henceforth using 4.13 and 12.7 ppm as the concentrations of those samples. We shall focus on the data from the 15-ppm sample as it appears to be free from cluster effects and gives essentially the same results as the 5-ppm sample with the exception of better precision, presumably due to stronger signals. Vochten *et al.* show their susceptibility data only as a function of $1/T$ which makes it impossible to determine the high-temperature data, but they state that they can fit their data from 300 K down to 12 K with the sum of a Curie-Weiss term and a temperature independent term and quote a Weiss temperature of 3.4 ± 0.3 K and an effective magnetic moment of $(3.99 \pm 0.04)\mu_B$. The Weiss temperature and moment are both somewhat higher than the values calculated from the Hirst model, but fall within the uncertainties of the calculation.

Although the model calculation gives fair agreement with the data as analyzed by Vochten *et al.*, interpretation of the data in an alternate manner improves the agreement. We are concerned about two points: (1) we suspect the experimental uncertainties, may be larger than stated, and (2) we worry about the procedure of determining the impurity concentrations for the two most dilute alloys by scaling the susceptibilities relative to the most concentrated sample.

Since the impurity susceptibility is proportional to the number of impurity atoms contributing to the susceptibility, determination of the effective magnetic moment is limited by the precision to which the concentration of *isolated* impurities is known. Since Vochten *et al.* were willing to adjust the impurity concentrations by 16% with their scaling procedure, we would suppose that the uncertainty in the determination of the impurity concentration may be as high as 16% (Vochten *et al.* give no uncertainties for their concentration analysis). A 16% error in the concentration results in an 8% error in the determination of the effective magnetic moment. The uncertainties quoted for the susceptibility parameters appear to reflect only the uncertainties due to data scatter, as is further evidenced by the fact that the size of the temperature independent contributions to the susceptibilities quoted for the three samples are by no means proportional to the concentrations to within the uncertainties quoted. The strong interdependence between the parameters in a fitting procedure also seems to have been neglected in stating the uncertainties. An error in determination of the Weiss temperature, for example, strongly affects the value determined for the moment since the low-temperature data are implicitly weighted strongly in a fit to a Curie-Weiss law.

The scaling procedure used to determine the impurity concentration in the more dilute alloys tacitly seems to us to assume that the analyzed concentration of the 112-ppm sample is all in the form of isolated impurities—despite the experimental evidence that the 112-ppm sample *does* suffer from clustering. We view the fact that the percentages by which the concentrations of the more dilute alloys were scaled are nearly the same (−15% and −17%) as further evidence that a preferable interpretation of the data is that the 112-ppm sample has about 16% of its impurity concentration in the form of clusters. In any event, it seems to us that the possibility of this alternate interpretation means that the moment determined by the experiment is subject to considerable uncertainty.

In view of these objections to the analysis of the bulk susceptibility data, we have reanalyzed the data assuming the concentration of the "12.7-ppm" alloy is 15 ppm. The effective magnetic moment is then $(3.7 \pm 0.4)\mu_B$, where the uncertainty is only our estimation as to the minimum experimental uncertainties reflected by the data. We have plotted the rough form of the data on Fig. 4 by using the expression derived from our analysis of this experiment, given as Eq. (29) below, for the susceptibility of 12 to 300 K and the expression given as Eq. (30) below, derived from analysis of published data obtained in a separate experiment by Hoeve and Van Ostenburg[30] at higher temperatures, for the temperature range of 300 to 700 K. The expressions used for the numerical fit to the susceptibility data are

$$\chi = \frac{(3.67)^2 \mu_B^2 N}{3k_B} \frac{1}{T+3.4} + 12.4 \times 10^{-4} , \quad (29)$$

$$\chi = \frac{(4.00)^2 \mu_B^2 N}{3k_B} \frac{1}{T+2.9} + 3.6 \times 10^{-4} . \quad (30)$$

The agreement shown in Fig. 4 is well within the experimental and calculation uncertainties. Note particularly that although experimental uncertainties preclude a definite determination, the data do appear to show the departure from the single Curie-Weiss-plus-temperature-independent law at high temperatures from the $F=1$ and 2 states.

3. *Anomolous low-temperature susceptibility*

Vochten *et al.* plot the data obtained from the 15-ppm alloy as a function of $1/T$ to demonstrate that at temperatures below about 10 K the susceptibility deviates markedly from the high-temperature Curie-Weiss-plus-temperature-independent form. It appears that at least part of the low-temperature susceptibility is due to a moment with a Weiss temperature of essentially zero. The low Weiss temperature is evidenced by the temperature dependence of the susceptibility and the ease with which the moment is saturated by magnetic field. We comment further on this problem in Sec. VI.

4. *Hyperfine fields*

There have been two studies of the hyperfine field at the nucleus of ^{51}Cr in Cu. The first was by Williams, Campbell, Sanctuary, and Wilson,[32] the second by Brewer.[33] The method was the measurement of γ-ray anisotropy produced by the alignment of the ^{51}Cr nucleus at temperatures of order $(5-15)\times10^{-3}$ K in applied magnetic fields of tens of kOe. The experiments are interpreted on the assumption that the ^{51}Cr nuclear magnetic moment is aligned by the Cr electron magnetic moment through the hyperfine coupling. Brewer finds a hyperfine field of -153 kG.

For our model of Cr, there should also be an electric quadrupole contribution to the alignment since when the electron magnetic moment is aligned the orbital wave function would produce an alignment of the electric field gradient at the ^{51}Cr nucleus ($I=7/2$). Unfortunately the ^{51}Cr electric quadrupole moment has not been measured. However, one can get an idea of the size of the alignment by examining the quadrupole splittings of ^{57}Fe in the $(3d)^6$ configuration (Fe^{2+}), the hole equivalent of Cr $(3d)^4$. Ingalls[34] has analyzed Fe^{2+} in a number of systems. The quadrupole splittings are of the order 20–40 MHz. This is quite comparable to the 30 MHz precession frequency of ^{51}Cr in 153 kG.

It is straightforward to estimate the hyperfine field from our picture. Using Eq. (27) with $\langle S_z\rangle=-2$, $\langle L_{ez}\rangle=-1$, $\alpha=1$, and $k=0.84$, taking Narath's theoretical value of $H_L=325$ kOe, and assuming $H_S=-50$ kOe (the value deduced for *Cu*Mn), we get

$$H_{\rm hf}^{\rm sat}=-470\ \text{kOe}\ . \tag{31}$$

If, on reanalysis of the ^{51}Cr alignment data, one could rule out a quadrupole contribution to the alignment, there would be a disagreement between our model and experiment. If there were found to be both a quadrupole alignment and a magnetic alignment, one could compare the magnetic alignment with the prediction of Eq. (31).

C. *Cu*Fe

1. *Bulk magnetic susceptibility and satellite data*

We analyze Fe in both $3d^6$ and $3d^7$ configurations. We begin following Hirst with the $3d^6$ configurational ground state with T_2 symmetry [see Fig. 1(a)]. We calculate an effective magnetic moment of $4.8\mu_B$, assuming the orbital reduction factor is 1. If the orbital angular momentum is completely quenched ($k=0$), the calculated effective moment is $4.1\mu_B$. Steiner *et al.*[21] experimentally determined the value to be $(3.54\pm0.08)\mu_B$. For the calculated value of 4.1 μ_B which corresponds to $k=0$, to be correct, the experimental concentration must be in error by more than 30%; the value of $4.8\mu_B$ which corresponds to $k=1$, requires that the concentration be in error by more than 90%. Since k is expected to be closer to 1 than 0, we conclude that the experimental concentration is probably not in error enough to make the experimentally determined moment consistent with the $3d^6$, T_2 symmetry ground state.

The T_2 ground state has a temperature independent contribution to the spin susceptibility of the form of Eq. (10); as a consequence the NMR satellite splittings would be expected to deviate from the low-temperature Curie-Weiss law by about 30% at 300 K. Boyce and Slichter[13,14] detected no deviation from a Curie-Weiss law. The experimental uncertainties were sufficiently small that such a large deviation should have been detected.

We next try reversing the sign of the crystal field within the $3d^6$ configuration as we did for *Cu*Cr [Fig. 1(a) with Δ negative]. The ground state then has E symmetry with the smaller temperature independent contribution to the susceptibility of the form of Eq. (11); however the effective magnetic moment calculated for this ground state is $4.5\mu_B$, which would require a 60% error in the experimental concentration.

We conclude that the $3d^6$ assignment must be incorrect. The $3d^5$ assignment corresponds to that of *Cu*Mn which has an effective magnetic moment much larger than *Cu*Fe. We therefore try the $3d^7$ configurational assignment.

With Hirst's assignment of the crystal field sign the $3d^7$ configurational ground state has T_1 symmetry [Fig. 1(b) with Δ negative] with an effective magnetic moment of about the right size, but the temperature independent contribution of the spin-orbit split

ground state is again large. The NMR satellite data would be expected to show a 70% deviation from the low temperature Curie-Weiss law at 300 K which was not observed.

Finally we reverse the sign of the crystal field within the $3d^7$ configuration so that it agrees with the sign which successfully explained the *Cu*Cr data [Fig. 1(b)] and find we are above to obtain a reasonable fit to the *Cu*Fe data also. The ground state has A_2 symmetry. The effective magnetic moment is calculated to be $3.5\mu_B$, in excellent agreement with the experimental value of $(3.54 \pm 0.08)\mu_B$.

We assume that the orbital angular momentum and spin-orbit coupling parameter are reduced to 80% of their free ion values, similar to the reduction deduced for *Cu*Cr, and use the observed bulk susceptibility to estimate the size of the crystal-field splitting. The value obtained is of the order expected. Using the estimated value of the crystal-field splitting we compute the deviation from a Curie-Weiss law expected for the NMR satellite data and find it is consistent with the data.

From Appendix B we have that the ratio of the temperature independent contribution to the susceptibility to the temperature dependent contribution is

$$\frac{\chi_{\mathrm{TI}}}{\chi_{\mathrm{TD}}} = \frac{2k(2\Delta k - 3\lambda)k_B}{5\Delta(5\Delta - 2k\lambda)}(T+\theta) \ . \tag{32}$$

The observed ratio is $4.348 \times 10^{-4}(T+\theta)$.[31] The Fe^+ free ion has a spin-orbit coupling parameter of -119 cm^{-1}; we assume it is reduced to -95 cm^{-1} and use $k=0.8$. Equating Eq. (32) with the experimentally determined ratio, we solve for Δ and find $\Delta = 249$ cm^{-1}; therefore the energy splitting from the A_2 ground state to the first excited crystal-field-split state is obtained from $5\Delta = 1245$ cm^{-1}. The splitting is the equivalent of about 1800 K which is of the order of the size of crystal field expected.[18]

The ratio of the temperature independent contribution to the spin susceptibility to the temperature dependent spin susceptibility is just:

$$\frac{\chi^S_{\mathrm{TI}}}{\chi^S_{\mathrm{TD}}} = -\frac{4\lambda k k_B(T+\theta)}{25\Delta^2} \ . \tag{33}$$

Evaluating Eq. (33) with $\theta = 28$ K at $T = 300$ K, we find the ratio to be 4.5%. While the assumption that the NMR satellite data have no temperature independent contribution is certainly possible within the experimental uncertainty, the addition of this small, temperature independent term actually improves the fit to Boyce and Slichter's data.

2. *Hyperfine field data*

Steiner *et al.*[31] have analyzed the Mössbauer and bulk susceptibility data and conclude $H_S = -50$ kOe and $H_L = 470$ kOe. They analyzed the data assuming that the temperature independent contributions to the local and macroscopic susceptibility are entirely due to the orbital susceptibility and the temperature dependent contributions are due to the spin only. As can be seen from Appendix B with $k=0.8$, $\lambda = -95$ cm^{-1} and $\Delta = 249$ cm^{-1}, the spin susceptibility contributes about 28% of the temperature independent susceptibility and the orbital susceptibility contributes about 11% of the temperature dependent susceptibility. Using

$$\begin{aligned} \chi_{\mathrm{mac}} &= -\frac{1}{H}(2\langle S_z\rangle + \langle L_z\rangle) \ , \\ \chi_{\mathrm{loc}} &= -H_S\langle S_z\rangle/SH - H_L\langle L_z\rangle/LH \ , \end{aligned} \tag{34}$$

to deduce

$$\chi_{\mathrm{loc}} = \chi^S_{\mathrm{mac}}(H_S) + \chi^L_{\mathrm{mac}}(H_L) \ , \tag{35}$$

we find

$$\begin{aligned} \chi^{\mathrm{TI}}_{\mathrm{loc}} &= \chi^{\mathrm{IT}}_{\mathrm{mac}}[0.28(H_S) + 0.72(H_L)] \ , \\ \chi^{\mathrm{TD}}_{\mathrm{loc}} &= \chi^{\mathrm{TD}}_{\mathrm{mac}}[1.11(H_S) - 0.11(H_L)] \ . \end{aligned} \tag{36}$$

Using the values calculated by Steiner *et al.* from the data for χ_{loc} and χ_{max} we have $\chi^{\mathrm{TI}}_{\mathrm{loc}}/\chi^{\mathrm{TI}}_{\mathrm{mac}} = 470$ kOe and $\chi^{\mathrm{TD}}_{\mathrm{loc}}/\chi^{\mathrm{TD}}_{\mathrm{mac}} = -151$ kOe. Substituting these values into Eq. (35) and solving, we find $H_L = 679$ kOe, which agrees somewhat better with Narath's[24] calculated value of 600 kOe than the value of 470 kOe given by Steiner *et al.*, and $H_s = -69$ kOe comparable to the value found in Mn, and well within Narath's estimate of -25 kOe $\geq H_s \geq -140$ kOe.

When Hirst[35] analyzes the hyperfine fields in terms of the $3d^6$ configuration with a T_2 symmetry ground state, he finds it necessary to assume that k is less than 0.4 and the best fit value is $k=0$. He states that such a great orbital angular momentum reduction is too much to explain by the usual admixture of neighboring atomic wave functions. He postulates that a dynamic Jahn-Teller effect is present which has the effect of reducing the effective orbital angular momentum. We find it equally satisfying to assume that the ground state has its orbital angular momentum quenched by the crystal field.

VI. OTHER RELATED EXPERIMENTS

A. Magnetic susceptibility at low temperatures

In their studies of magnetic susceptibility, Vochten, Labro, and Vynckier report that their data fit a Curie-Weiss law down to about 10 K, but the experimental values below 10 K are higher. In Fig. 5, we have plotted $1/\chi$ vs T (obtained by reading data from their Fig. 2) to illustrate their point. This result is quite surprising on both theoretical and experimental

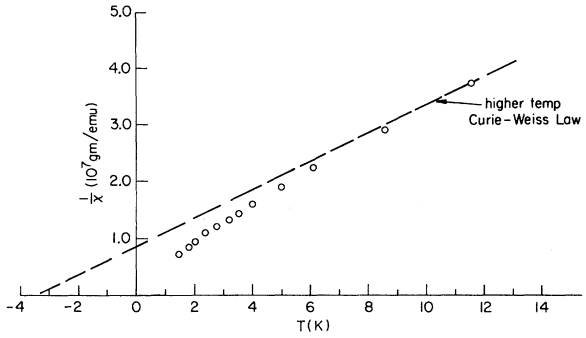

FIG. 5. Inverse of magnetic susceptibility vs temperature, showing the deviation from a Curie-Weiss law observed by Vochten, Labro, and Vynckier (Ref. 29) at low temperatures.

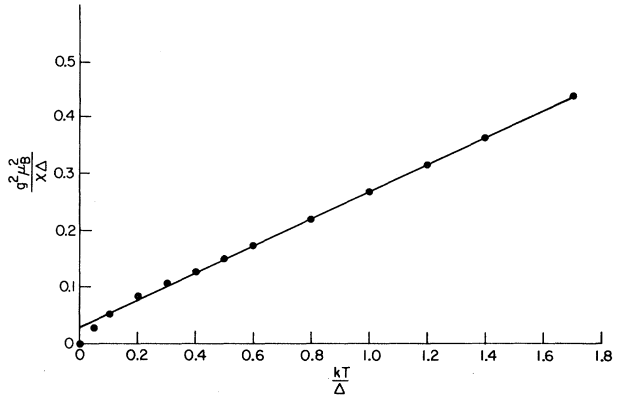

FIG. 6. Inverse of the theoretical value of magnetic susceptibility vs temperature, both in dimensionless units, for an effective angular momentum $F=3$, whose degeneracy is split by a cubic spin Hamiltonian into a singlet, and two triplets. Δ is the splitting between the two triplet states. It is assumed that one of the triplet states is the ground state. Note that for kT/Δ greater than about 0.2 the data simulate a Curie-Weiss law closely, though at low kT/Δ they go over to a Curie law, much like the data of Fig. 5.

grounds. Theoretical calculations show that the Kondo susceptibility is well approximated by a Curie-Weiss law except at the *very* lowest temperatures. Even there the deviation is opposite to that found by Vochten, Labro, and Vynckier. The experimental results on CuFe, also believed to be a Kondo system, are in excellent agreement with the theoretical prediction of a Curie-Weiss law. In the case of CuFe pairs of iron atoms have a lower Kondo temperature than isolated iron atoms so that the presence of pairs causes the measured susceptibility to have a strongly temperature dependent term well below the Kondo temperature of isolated Fe atoms. This term is identified as coming from clumps of two or more atoms by studies in which Fe concentrations are varied. Vochten, Labro, and Vynckier argue that the deviations are not the result of clumping effects since they get identical results for a sample containing 5 ppm of Cr as for a sample containing 15 ppm.

We have found that it is possible to simulate the results of Vochten, Labro, and Vynckier by assuming that instead of having a Kondo effect, the sevenfold degenerate Cr ground state is split by a Hamiltonian of cubic symmetry. Such a coupling gives three energy levels: a singlet and two triplets. If the sign of the coupling puts the singlet highest and one of the triplets lowest, the susceptibility varies with temperature as shown in Fig. 6. (In Fig. 6, Δ is the crystal splitting of the middle triplet state from the lowest triplet state.) (A cubic splitting of this form but *opposite sign* arises from treating spin-orbit coupling to second order in the spin-orbit coupling constant. We do not know a mechanism to provide the sign coupling we would need.) The form of the resultant susceptibility is much like that of Labro *et al.* In addition, there could be a Kondo effect of the ground triplet, or its energy could be split further by a Jahn-Teller distortion. Thus there are several possible explanations of the low-temperature susceptibility results. (Symko has told us that he likewise finds the susceptibility to be much more strongly temperature dependent below 1 K than would be implied by a Curie-Weiss law with Kondo temperature of 3 K such as implied by our satellite data or the high-temperature susceptibility data.)

We believe there are sufficient uncertainties in knowledge of the low-temperature susceptibility of isolated Cr atoms in Cu that we cannot select among the various suggested explanations of the susceptibility data currently in hand. Careful study of the concentration and temperature dependence of the magnetic susceptibility are clearly very important to determine the functional form of the magnetic susceptibility below 1 K.

B. Satellites at low temperatures and high magnetic fields

Azevedo, Follstaedt, and Narath[36] have performed an important test of the *Cu*Cr model by studying the satellite splittings at low temperatures (1.08 K) and high magnetic fields (up to 120 kG). At such low temperatures and high fields, the Cr magnetization should be saturated. In low magnetic fields, the thermal average of the Cr spin S_z is given by

$$\langle S_z\rangle = -a\frac{g\mu_B J(J+1)}{3k_B(T+T_k)}H \ ,$$

where μ_B is the Bohr magneton. Whereas the saturated value in high field is given by

$$\langle S_z\rangle_{\rm sat} = -aJ \ ,$$

where "a" is defined by the relation

$$\langle S_z\rangle = a\langle J_z\rangle$$

a relationship which follows from the Wigner-Eckart theorem ($a=2/3$ for our model). Therefore, the ratio of satellite splittings at a known low field to the saturated splitting gives one the product $g(J+1)$. Using the satellite labeled "B", the value $J=3$, the data of Azevedo *et al.* we find $g=1.15\pm0.03$, which, though slightly larger than our value of $g=1.05\pm0.09$, gives in our judgement a strong confirmation of the ionic model.

In the previous section we pointed out that a possible explanation of the mysterious low-temperature susceptibility results is the existence of cubic crystal splitting of the $J=3$ state. We have explored the effect of such a splitting on the shape of the curve of satellite splitting versus magnetic field. We have also explored the shape of the same saturation curve assuming only a Kondo effect. Unfortunately, there is no rigorous treatment of the Kondo effect at large magnetic fields. We were forced therefore to assume a Brillouin function for $J=3$ with T replaced by $T+\theta$. We find that we can get a better fit of the saturation curve using the crystal-field fit, but that even our crude approach to saturation using the Kondo effect gives a fit which must be considered satisfactory considering its lack of rigorous theoretical justification.

Azevedo, Follstaedt, and Narath have also measured the spin-lattice relaxation time of satellite B. They find that its field dependence has the same form as that of other Kondo systems (WCo). They use a scaling procedure involving the T_1's measured for WCo and CuCr to deduce that the Kondo temperature of CuCr is 3.3 K, a value close to that which we find. They therefore favor the concept that CuCr has a real Kondo effect, not a crystal-field effect.[37]

Thus our data at low field and high temperature together with that of Azevedo, Follstaedt, and Narath at high field and low temperature are internally consistent, all supporting the ionic model of Cr with $J=3$, $g\cong1$, and a Kondo effect wtih $T_k\cong3$ K.

C. Transmission electron spin resonance

Transmission electron spin resonance (TESR) has been used to study CuMn,[38] CuCr,[39] and CuFe.[40] In this technique the magnetic impurity is observed indirectly by its effect on the conduction electron spin resonance. For CuMn, the Mn resonance has also been observed directly through conventional reflection electron spin resonance.

The presence of an impurity produces scattering of a conduction electron. Even nonmagnetic impurities can in the process flip the electron spins. Such a process gives an ESR line breadth proportional to the impurity concentration. For a nonmagnetic impurity the impurity scattering line breadth is independent of temperature.

When the impurity is magnetic we expect two extra effects. Since the TESR is observed under the action of an applied magnetic field, the impurity moments are somewhat polarized, giving rise to Weiss field acting on the conduction electrons resulting in a g shift of the TESR proportional to the impurity concentration and susceptibility. That field displaces the TESR from its field in the pure host. Also, the spin-flip scattering cross section becomes temperature dependent, growing at low temperatures as a result of the Kondo effect. (The Kondo effect acts much like a narrow scattering resonance located at the Fermi energy.)

Both CuCr and CuFe have such a behavior. Both display TESR linewidths proportional to impurity concentration, the linewidth growing somewhat at low temperatures. In CuCr the g shift from its value in pure Cu is proportional to Cr concentration, and roughly follows the Cr susceptibility with temperature. In CuFe no g shift is observed, probably because the high Kondo temperature ($T_k\cong28$ K) makes the CuFe susceptibility so small that the polarization of the Fe atom is negligible.

If the impurity itself has a g factor close to that of the conduction electrons ($g\cong2$), the conduction electron and impurity may act like a strongly coupled system. At sufficiently low temperatures, if the impurity Kondo temperature is low enough the magnetic susceptibility of the impurity completely dominates the response, and the width of the resonance line becomes independent of concentration. The concentration-independent line breadth is one hallmark of the closely coupled case. The second hallmark is that the TESR g factor at low temperature goes to that found for the impurity by reflection experiments. For CuMn both hallmarks of the coupled systems are observed. The reflection and transmission experiments are completely consistent with the ionic model of Mn being $g=2$, d^5 configuration with $S=5/2$, $L=0$.

Monod and Schultz assumed in their analysis of CuCr that it too was a strongly coupled system with $g\cong2$, in sharp contrast with our deduction that $g\cong1$. However, their assumption is not necessary since *neither* hallmark of the coupled system is observed (the Cr resonance has never been seen in reflection, and the line breadth is proportional to concentration at even the lowest temperatures). Thus there is no reason to assume that the Cr g value is two as would be required by a coupled system.

The analysis of Ritter and Silsbee of CuFe examines various models of the Fe atom, including ionic models for $3d^6$ and $3d^7$, and both signs of crystal field. They are not able to make a conclusive determination of the electronic structure. They likewise assume a strongly coupled system with iron having a $g=2$. Their data likewise does not require such an assumption since neither hallmark of the strongly coupled system is present. They neither confirm nor

rule out our picture.

We therefore find that reflection ESR and TESR confirm the ionic model for *Cu*Mn, but do not distinguish various models for *Cu*Cr or *Cu*Fe.

D. Linewidths of *Cu*Fe satellites

Alloul and Ishii[41] have observed a strong temperature dependence of the width of satellites B and M in the *Cu*Fe system. In seeking an explanation, they also propose that spin-orbit coupling in the Fe atom plays a role. They predict a temperature independent contribution to $\Delta K/K$ as a result, and reanalyze their data to conclude that the size of the temperature independent $\Delta K/K$ for satellite B is 0.15 ± 0.05. This is somewhat larger than we conclude in Sec. V C from our analysis of the data. The result is very much dependent on the Kondo temperature one assumes.

Alloul and Ishii utilize the Friedel-Anderson model to analyze their result. They find rough agreement as to magnitude, but the wrong sign for the temperature independent term. They attribute the temperature independent term of $\Delta K/K$ to the temperature independent part of the *orbital* susceptibility.

As we remarked earlier, we do not believe the Friedel-Anderson approach would be able to explain the great difference between *Cu*Fe and *Cu*Cr. The ionic model is able to explain correctly not only the magnitudes but also the signs of the temperature independent terms.

VII. CONCLUSIONS

The observation of temperature independent contributions to the bulk magnetic susceptibility and NMR satellite data require the inclusion of nondegenerate orbital states in the model used for explaining the nature of the isolated Cr impurities in dilute *Cu*Cr alloys; further, the temperature independent contribution to the NMR satellite splittings, which are proportional to the spin susceptibility, requires that there be spin-orbit coupling present. The only model of $3d$ impurities in nonmagnetic metallic hosts which has been worked out in sufficient detail to include such fine structure is the ionic model proposed by Hirst. Our data support his model, though the details are somewhat different. Attempting to understand the experimental evidence on *Cu*Cr, *Cu*Mn, and *Cu*Fe in terms of the ground state configurations proposed by Hirst, we are forced to conclude that his assignments are incorrect. By choosing the sign of the crystal field present at the impurity sites opposite of that proposed by Hirst, we find good agreement between the model and the experimental evidence when we assign the $3d^4$, $3d^5$, and $3d^7$ configurations to Cr, Mn, and Fe, respectively. These configurations agree with those proposed by Hirst except for Fe which he considers to be $3d^6$. Hirst[8] expects a jump in the regular progression of $3d^n$ ground-state configurations such as we find between Mn and Fe since he believes Cu to be $3d^{10}$, but he proposed that the jump occurs at Ni. Cohen and Slichter[42] also find a jump between Mn and Fe when they fit NMR satellite data to a potential scattering model. They find 4.0, 5.0, and 7.0 d electrons for Cr, Mn, and Fe, respectively. Johnson, Vvedensky, and Messmer's[43] cluster calculations also agree. The apparent integral jump in the number of d electrons on the impurity is additional evidence that the ground-state level widths are much smaller than the virtual bound state widths calculated in a Friedel scattering model or a Hartree-Fock approximation to the Anderson model and thus further confirms Hirst's model.

In Table IV we summarize the configurations and model parameters which we have determined or estimated for the three alloys.

We believe that our satellite data and the low-temperature, high-field data of Azevedo, Follstaedt, and Narath verify the theoretical description of Cr, including the facts that $J=3$ and $g \cong 1$. Still unresolved, however, is the behavior of the Cr ground state at temperatures below about 1 K. In particular,

TABLE IV. Summary of model configurations and parameters.

Alloy	Configuration	L	S	Ground state symm.	Crystal field Δ (cm^{-1})	Spin orbit λ (cm^{-1})	Orbital reduc. k	$\frac{H_s}{2S}$ (kOe)	$\frac{H_L}{L}$ (kOe)	μ_{eff} (μ_B)	ρJ
*Cu*Cr	$3d^4$	2	2	T_2	· · ·	48(32)	0.84(19)	−40[a]	225[a]	3.4(4)	−0.11
*Cu*Mn	$3d^5$	0	5/2	A_1	· · ·	· · ·	· · ·	−56	· · ·	4.8	−0.33
*Cu*Fe	$3d^7$	3	3/2	A_2	249[b]	−95[c]	0.8[c]	−69	679	3.5	−0.31

[a] Speculation only. See Sec. A. [b] Calculated from assumed values of λ and k. [c] Estimated at 80% of free ion values.

the anomalous behavior of the magnetic susceptibility raises the question of whether or not *Cu*Cr truly has a Kondo effect, and if so what is the Kondo temperature. Extension of the low-temperature susceptibility measurements to check more extensively for possible concentration dependent effects is highly desirable.

A reexamination of the low-temperature Cr nuclear alignment data to see whether or not there is a quadrupole alignment would provide an independent test of our claims because our model requires a quadrupole coupling in order to explain the observed nuclear alignment.

This research was supported in part by the U.S. Department of Energy under Contract No. DE-AC02-76ER01198.

APPENDIX A: TEMPERATURE DEPENDENCE OF NMR SATELLITES

In this Appendix we show that the temperature dependence of the NMR satellite splittings ΔK is proportional to the spin susceptibility of the impurity, i.e.,

$$\frac{\Delta K}{K} = g(\vec{r})\chi^s(T) \ , \tag{A1}$$

where $g(\vec{r})$ is determined by the spatial dependence of the conduction electron polarization and is not a function of temperature. We consider only the part of ΔK due to the polarization of the conduction electrons through the Fermi contact interaction, which in the magnetic alloys is nearly all of ΔK for the magnetic field strengths commonly used in NMR.

We use the general form of the mixing interaction[21]

$$H_{\rm mix} = \sum_{\substack{km\sigma \\ k'm'\sigma'}} I_{kk'} a_{m\sigma} a_{m'\sigma'}^{\dagger} c_{k'm'\sigma'}^{\dagger} c_{km\sigma} \ , \tag{A2}$$

where the operator $a_{m\sigma}^{\dagger}$ creates an impurity electron with z component of angular momentum m and spin σ and the operator $c_{km\sigma}^{\dagger}$ creates a conduction electron with wave vector magntiude k, z component of angular momentum m and spin σ. The Fermi contact interaction between the conduction electrons and a host nucleus which is a neighbor of the impurity is given by

$$H_{en} = \frac{8\pi}{3}\gamma_e \hbar \mu_z \sum_{i=1}^{N} S_{zi}\delta(\vec{r}_i - \vec{R}) \ , \tag{A3}$$

where γ_e is the electron gyromagnetic ratio, μ_z is the z component of the nuclear magnetic moment, $\vec{R}$ is the position of the nucleus, and the sum over i is a sum over the N conduction electrons specified by positions $\vec{r}_i$. In second quantization notation Eq. (A3) may be written

$$H_{en} = \frac{8\pi}{3}\gamma_e \hbar \mu_z \sum_{\substack{\vec{k}\sigma \\ \vec{k}'\sigma'}} \psi_{\vec{k}'}^{*}(\vec{R})\psi_{\vec{k}}(\vec{R})\sigma\delta_{\sigma\sigma'} c_{\vec{k}'\sigma'}^{\dagger} c_{\vec{k}\sigma} \ . \tag{A4}$$

(For a discussion of a similar calculation which clarifies many of the details of this calculation, see Ref. 44.) Ordinarily one would take the electrons to be in Bloch states, $u_R(\vec{r})e^{i\vec{k}\cdot\vec{r}}$. We will take the states to be plane wave states instead, thus neglecting the large amplitude of the electron wave function near the nuclei as expressed by the $u_{\vec{k}}(\vec{r})$ factor. Since it is only the ratio of ΔK to K which is to be calculated this approximation should be reasonable. We then express the plane wave states as spherical waves, i.e., we assume they are in states of definite l, m about the impurity position. Equation (A4) then becomes

$$H_{en} = \frac{8\pi}{3}\gamma_e \hbar \mu_z \sum_{\substack{km\sigma \\ k'm'\sigma'}} Y_{2m'}^{*}(\hat{R})\, Y_{2m}(\hat{R})\, v_{k'}(R) v_k(R)\sigma\delta_{\sigma\sigma'} c_{k'm'\sigma'}^{\dagger} c_{km\sigma} \ , \tag{A5}$$

since the impurity moment complex couples only to d electrons, where $v_k(r)$ is the radial free electron d function with wave vector of magnitude k.

Let $|\alpha\rangle$ be the exact many-electron states of the impurity moment in the absence of $H_{\rm mix}$; let $|\beta\rangle$ be the exact many-electron states of the conduction electrons in the absence of H_{en}. The energy of interaction between the impurity moment and the neighboring nucleus is

$$\Delta E_{\alpha\beta} = \sum_{\alpha'\beta'} \frac{\langle\alpha\beta|H_{\rm mix}|\alpha'\beta'\rangle\langle\alpha'\beta'|H_{en}|\alpha\beta\rangle}{E_{\alpha\beta} - E_{\alpha'\beta'}} + \text{c.c.} \ . \tag{A6}$$

Substituting Eqs. (A2) and (A5) into Eq. (A6) and simplifying we have

$$\begin{aligned}\Delta E_{\alpha\beta} &= \frac{8\pi}{3}\gamma_e \hbar \mu_z \sum_{\substack{km\sigma \\ k'm'\beta'}} I_{kk'}\langle\alpha|a_{m\sigma}^{\dagger}a_{m'\sigma}|\alpha\rangle\langle\beta|c_{k'm'\sigma}^{\dagger}c_{km\sigma}|\beta'\rangle\langle\beta'|Y_{2m'}^{*}(\hat{R})\,Y_{2m}(\hat{R})\,v_{k'}(R)v_k(R)\sigma c_{km\sigma}^{\dagger}c_{k'm'\sigma}|\beta\rangle + \text{c.c.} \\ &= \frac{16\pi}{3}\gamma_e \hbar \mu_z \sum_{mm'\sigma}\langle\alpha|a_{m\sigma}^{\dagger}a_{m'\sigma}|\alpha\rangle\, Y_{2m'}^{*}(\hat{R})\,Y_{2m}(\hat{R})\,\sigma \sum_{\beta' kk'} \frac{\langle\beta|c_{k'm'\sigma}^{\dagger}c_{km\sigma}|\beta'\rangle\langle\beta'|c_{km\sigma}^{\dagger}c_{k'm'\sigma}|\beta\rangle v_{k'}(R)v_k(R)}{E_\beta - E_{\beta'}} I_{kk'}\end{aligned} \tag{A7}$$

We now note that

$$\sum_{mm'\alpha} \sigma a^{\dagger}_{m\sigma} a_{m'\sigma} Y^{*}_{2m'}(\hat{R})\, Y_{2m}(\hat{R}) \tag{A8}$$

in second quantization notation for

$$\sum_{i=1}^{N} s_{zi}\delta(\hat{r}_i - \hat{R}) \ , \tag{A9}$$

where the sum is over the N impurity d electrons with angular position specified by $\hat{r}_i$. We approximate that the conduction electron states are the same as in the absence of a magnetic field; then

$$\langle\beta| c^{\dagger}_{k'm'\sigma} c_{km\sigma} |\beta'\rangle = 0 \ , \tag{A10}$$

unless $|\beta\rangle$ contains an electron with quantum numbers $k'm'\sigma$ and $|\beta'\rangle$ contains an electron with quantum numbers $km\sigma$, in which case it equals one. Let p_α be the probability that $|\alpha\rangle$ is occupied and p_k be the probability that the conduction electron state with wave vector magnitude k is occupied. The thermal average of (A7) becomes

$$\Delta E_{\alpha\beta} = A_0 \sum_{\alpha} p_\alpha \left\langle \alpha \middle| \sum_i S_{zi}\delta(\hat{r}_i - \hat{R}) \middle| \alpha \right\rangle \ , \tag{A11}$$

where

$$A_0 = \frac{16\pi}{3}\gamma_e \hbar \mu_z \times \sum_{k,k'} I_{kk'} \frac{p_k(1-p_{k'}) v_{k'}(R) v_k(R)}{E_k - E_{k'}} \ . \tag{A12}$$

The unit vector $\hat{R}$ points towards a particular neighbor in a shell. Let there be N_s atoms in a shell, designated by $\hat{R}_n$ where $n = 1, \ldots N_S$. In a single crystal, the spectra of a given shell consist of a small number of closely spaced lines. In a powder, these lines are smeared together so that each shell gives rise to a single satellite. Thus, to get the position of a satellite for a powder, we must average over all orientations of $\hat{R}$. To do so we have that the average of $\langle\alpha|\sum_i s_{zi}\delta(\hat{r}_i - \hat{R}_n)|\alpha\rangle$ for a shell is

$$\left\langle \alpha \middle| \sum_i s_{zi}\delta(\hat{r}_i - \hat{R}_n) \middle| \alpha \right\rangle_{\rm av} = \frac{1}{N_s} \sum_{n=1}^{N_s} \left\langle \alpha \middle| \sum_i s_{zi}\delta(\hat{r}_i - \hat{R}_n) \middle| \alpha \right\rangle \cong \frac{1}{4\pi} \int d\Omega \left\langle \alpha \middle| \sum_i s_{zi}\delta(\hat{r}_i - \hat{R}) \middle| \alpha \right\rangle \ , \tag{A13}$$

where we replace the sum by an integral over solid angle Ω, and where the unit vector $\hat{R}$ roams over a sphere. Performing the Ω integral before evaluating the expectation value, we get

$$\left\langle \alpha \middle| \sum_i s_{zi}\delta(\hat{r}_i - \hat{R}_n) \middle| \alpha \right\rangle_{\rm av} = \left\langle \alpha \middle| \sum_i s_{zi} \middle| \alpha \right\rangle = \langle\alpha|S_z|\alpha\rangle \ . \tag{A14}$$

Therefore for a full shell

$$\Delta E_{\alpha\beta} = A_0 \sum_{\alpha} p_\alpha \langle\alpha|S_z|\alpha\rangle = A_0 \langle S_z\rangle \ . \tag{A15}$$

Although A_0 involves temperature (in the p_k's) the temperature dependence is negligible for the same reasons that the Knight shift K of a pure metal is temperature independent. Thus the temperature dependence of the satellite arises solely from $\langle S_z\rangle$. Equation (A15) implies that *all* satellite shells of a given impurity in a given host have the *same* temperature dependence of their splitting from the main line, in agreement with experiment for *Cu*Cr, *Cu*Mn, and *Cu*Fe.

APPENDIX B: SUSCEPTIBILITY CALCULATIONS

In this Appendix we describe the calculation of the magnetic susceptibility from the ionic model for the various configurations and give the formulas for the spin susceptibility and the total susceptibility. For those configurations of particular interest for this study, we give the calculation of the reduction of the effective magnetic moment due to the impurity electron-conduction electron mixing interaction.

A. Triplet ground state

If the crystal-field ground state is a triplet, the orbital angular momentum is unquenched and the crystal-field ground state degeneracy will be further split by the spin-orbit coupling. We calculate the susceptibility of the crystal-field ground state only, ignoring the excited crystal-field states which probably lie several thousand degrees above the ground state. Within the triplet ground state we write

$$H = H_{\rm so} + H_z \ , \tag{B1}$$

where

$$H_{\rm so} = \lambda \vec{L}\cdot\vec{S}; \quad H_z = \mu_B H(kL_z + 2S_z) \ , \tag{B2}$$

where k is an orbital reduction parameter which represents a reduction of the orbital angular momentum from that of the free ion due to the crystal environment (see Ref. 16). We have made use of the cubic symmetry and assumed that $\vec{H}$ lies along the z axis. Let

$$H_{\rm so}|FM\rangle = E_F|FM\rangle \ . \tag{B3}$$

To create states which are nearly eigenstates of H, we treat H_z as a perturbation of H_{so}:

$$|FM) = |FM\rangle + \sum_{F' \neq F} \frac{\langle F'M|H_z|FM\rangle}{E_F - E_{F'}} |F'M\rangle \quad \text{(B4)}$$

so that

$$H|FM) \approx E_F|FM\rangle + H_z|FM\rangle \ . \quad \text{(B5)}$$

To calculate the thermal average of S_z we evaluate the trace of S_z times the density operator. As discussed in Sec. II D, since the excited crystal-field states are far above the ground state, the Boltzman factor makes the contribution from these states small and we ignore their contribution, approximating the trace by a trace over the ground crystal-field state only:

$$\langle S_z\rangle \approx \left[\sum_F (2F+1)e^{-\beta E_F}\right]^{-1} \sum_{FM} \left[2 \sum_{F \neq F'} \frac{\langle FM|H_z|F'M'\rangle\langle F'M'|S_z|FM\rangle}{E_F - E_{F'}} - \beta\langle FM|S_z|FM\rangle\langle FM|H_z|FM\rangle\right] e^{-\beta E_F} \ . \quad \text{(B6)}$$

From Eq. (B6) we see that within the spin-orbit ground state the spin polarization has both a temperature dependent and a temperature independent term. The formula for the thermal average of L_z is obtained completely analogously to Eq. (B6) and is identical to it with L_z substituted for S_z everywhere in the expression. The susceptibility is obtained from

$$\chi^s = -\frac{2\mu_B N}{H}\langle S_z\rangle \ , \quad \text{(B7)}$$

$$\chi^{\text{tot}} = -\frac{\mu_B N}{H}(\alpha k\langle L_{ez}\rangle + 2\langle S_z\rangle) \ . \quad \text{(B8)}$$

We find it convenient to use a matrix transformation to obtain the matrix elements required to compute Eq. (B6). Designate

$$M_{ij} = \langle i|H_{so}|j\rangle \text{ with } |i\rangle = |LM_L SM_S\rangle \ . \quad \text{(B9)}$$

We define a matrix V:

$$M' = V^{-1}MV \quad \text{(B10)}$$

such that M' is diagonal. Since H_{so} simply couples the fictitious angular momentum $\vec{L}_e$ with the spin $\vec{S}$ to form a total fictitious momentum F, V is simply composed of Clebsch-Gordan coefficients and can be written down immediately. We define

$$Z^S_{ij} = \langle i|S_z|j\rangle, \quad Z^L_{ij} = \langle i|L_z|j\rangle \ ; \quad \text{(B11)}$$

$$Z^{S'} = V^{-1}Z_S V, \quad Z^{L'} = V^{-1}Z^L V \ ,$$

The last two matrices are the matrices required for Eq. (B6) and the analogous equation for L_z.

B. Doublet or singlet ground state

If the crystal-field ground state is a doublet or a singlet, the orbital angular momentum is quenched within the ground state. Some orbital susceptibility and some temperature independent spin susceptibility result from a mixing of the excited crystal-field states into the ground state by the applied magnetic field. We treat both the spin orbit and Zeeman interactions as perturbations on the crystal field. From group theory we know that the perturbing Hamiltonian, given as Eqs. (B1) and (B2) with $\alpha = 1$ since we are now using states of real angular momentum, connects an A_2 ground state only to the T_2 excited crystal-field states of an F state. (Refer to Fig. 1.) It also connects the E ground state to the excited T_2 states of a D state. We therefore treat both cases simultaneously. We designate an unperturbed ground state by $|im_s\rangle$ (i refers to A_2 or one of the E orbital states) and calculate the corrections to the ground states to second order:

$$|im_s) = |im_s\rangle + \sum_{FM} \frac{\langle FM|H|im_s\rangle}{E_i - E_F}|FM\rangle + \sum_{\substack{FM \\ F'M'}} \frac{\langle F'M'|H|FM\rangle\langle FM|H|im_s\rangle}{(E_i - E_{F'})(E_i - E_F)}|F'M'\rangle \ . \quad \text{(B12)}$$

We have written the T_2 excited states as $|FM\rangle$ because of the spin-orbit splitting withing the triplet state. We calculate the thermal average of L_z, again approximating with a trace over the ground crystal-field state only:

$$\langle L_z\rangle \approx \frac{1}{Z}\sum_{im_s}[(im_s|L_z|im_s) - \beta(im_s|L_z H|im_s)] \ . \quad \text{(B13)}$$

To second order in H

$$\langle L_z\rangle = \frac{1}{Z}\sum_{im_s}\Bigg[\overset{(1)}{\langle im_s|L_z|im_s\rangle} + 2\sum_{FM}\overset{(2)}{\frac{\langle im_s|L_z|FM\rangle\langle FM|H|im_s\rangle}{E_i-E_F}} + \sum_{\substack{FM\\F'M'}}\overset{(3)}{\frac{\langle im_s|H|FM\rangle\langle FM|L_z|F'M'\rangle\langle F'M'|H|im_s\rangle}{(E_i-E_{F'})(E_i-E_F)}} + 2\sum_{\substack{FM\\F'M'}}\overset{(4)}{\frac{\langle im_s|L_z|F'M'\rangle\langle F'M'|H|FM\rangle\langle FM|H|im_s\rangle}{(E_i-E_{F'})(E_i-E_F)}} - \beta\left[\langle im_s|L_zH|im_s\rangle + 2\sum_{FM}\frac{\langle im_s|L_zH|FM\rangle\langle FM|H|im_s\rangle}{E_i-E_F}\right]\Bigg] \quad \text{(B14)}$$

Equation (B14) appears rather formidable, but with an approximation and a few tricks it is easily evaluated. Since the spin-orbit splittings are much smaller than the crystal-field splittings, we ignore the differences in the energies of the excited state and let $E_i - E_F = E_i - E_{F'} = \Delta$. Since the excited states are composed of orbital states which are orthogonal to the ground state, S_z does not connect the ground and excited states. Consider the terms of Eq. (B14):

$$(1) = 0 \text{ since } L_z \text{ vanishes in the ground state} \quad . \quad \text{(B15)}$$

Since the sum in term (2) extends over all of the $|FM\rangle$ states, a change of basis to $|M_LM_S\rangle$ states is possible. Although the $|M_LM_S\rangle$ basis includes states in the ground state, and also states in the T_1 excited state for the crystal-field-split F states, the matrix elements of L_z between the ground state and these states vanish. Thus

$$(2) = -\frac{2}{\Delta}\sum_{\substack{im_s\\M_LM_S}}\langle im_s|L_z|M_LM_S\rangle\langle M_LM_S|H|im_s\rangle \quad . \quad \text{(B16)}$$

With the $|M_LM_S\rangle$ basis states the orbital and spin subspaces are separated and the operators L_z and S_z must appear in the trace to even powers or the trace vanishes. This allows immediate elimination of the majority of terms. Thus

$$(2) = -\frac{2(2S+1)\mu_B Hk\Sigma}{\Delta} \quad , \quad \text{(B17)}$$

where we have defined

$$\Sigma = \sum_{im_L}|\langle i|L_z^2|M_L\rangle|^2 \quad , \quad \text{(B18)}$$

$$(3) = 0 \quad , \quad \text{(B19)}$$

since after a change of basis to the $|M_LM_S\rangle$ states, it is impossible to form the L_z and S_z operators both to even powers

$$(4) = \frac{4\mu_B H\Sigma}{\Delta^2}TrS_z^2 \quad , \quad \text{(B20)}$$

$$(5) = 0 \quad , \quad \text{(B21)}$$

$$(6) = \frac{4\mu_B H\lambda\beta\Sigma}{\Delta}TrS_z^2 \quad . \quad \text{(B22)}$$

Collecting terms:

$$\langle L_z\rangle = -\frac{2\mu_B H\Sigma}{n_i}\left(\frac{k}{\Delta} - \frac{2S(S+1)\lambda}{3\Delta^2} - \frac{2S(S+1)\lambda\beta}{3\Delta}\right) \quad \text{(B23)}$$

where n_i is the orbital degeneracy of the ground state

$$\chi^L = \frac{4\mu_B^2 Nk}{n_i\Delta}\left(k - \frac{2S(S+1)\lambda}{3\Delta} - \frac{2S(S+1)\lambda}{3k_BT}\right) \quad . \quad \text{(B24)}$$

We obtain the spin susceptibility in a similar manner. The result is

$$\chi^s = \frac{4\mu_B^2 NS(S+1)}{3}\left(\frac{1}{k_BT} - \frac{2k\lambda\Sigma}{n_i\Delta^2}\right) \quad . \quad \text{(B25)}$$

Combining the spin and orbital susceptibilities

$$\chi^{\text{tot}} = 4\mu_B^2 N\left[\frac{S(S+1)}{3k_BT}\left(1 - \frac{2\lambda k\Sigma}{n_i\Delta}\right) + \frac{k}{n_i\Delta}\left(k - \frac{4S(S+1)\lambda}{3\Delta}\right)\right] \quad . \quad \text{(B26)}$$

*Now at Research Laboratories, Eastman Kodak Co., Kodak Park, Rochester, N.Y. 14650.
†Now at Department of Physics, University of Virginia, McCormick Rd., Charlottesville, Va. 22901.

[1]C. Zener, Phys. Rev. 81, 440 (1951).
[2]J. Kondo, Prog. Theor. Phys. (Kyoto) 32, 37 (1964).
[3]H. R. Krishna-murthy, K. G. Wilson, and J. W. Wilkins, Phys. Rev. Lett. 35, 1101 (1975).
[4]J. Friedel, Philos. Mag. 43, 153 (1952).
[5]P. W. Anderson, Phys. Rev. 124, 41 (1961).
[6]A. Blandin, J. Appl. Phys. 39, 1285 (1968).
[7]B. Coqblin and A. Blandin, Adv. Phys. 17, 281 (1968).
[8]J. R. Schrieffer and P. A. Wolff, Phys. Rev. 149, 491 (1966).
[9]J. R. Schrieffer and D. C. Mattis, Phys. Rev. 140, A1412 (1965).
[10]L. L. Hirst, Z. Phys. 241, 9 (1971); L. L. Hirst, in *Magnetism and Magnetic Materials—1974,* edited by C. D. Graham, G. H. Lander, and J. J. Rhyne, AIP Conf. Proc. No. 24 (AIP, New York, 1975), p. 11.
[11]C. P. Flynn, J. J. Peters, and C. A. Wert, Phys. Lett. 35A, 157 (1971); J. J. Peter and C. P. Flynn, Phys. Rev. B 6, 3343 (1972).
[12]T. J. Aton, T. S. Stakelon, and C. P. Slichter, Phys. Rev. B 21, 4060 (1980).
[13]J. B. Boyce and C. P. Slichter, Phys. Rev. Lett. 32, 61 (1974).
[14]J. B. Boyce and C. P. Slichter, Phys. Rev. B 13, 379 (1976).
[15]T. J. Aton, T. S. Stakelon, and C. P. Slichter, Phys. Rev. B 18, 337 (1978).
[16]D. C. Abbas, T. J. Aton, and C. P. Slichter, J. Appl. Phys. 49, 1540 (1978).
[17]D. C. Abbas, T. J. Aton, and C. P. Slichter, Phys. Rev. Lett. 41, 719 (1978).
[18]L. L. Hirst, Arch. Sci. 27, 279 (1974).
[19]Y. Yafet, Phys. Lett. 26A, 481 (1968).
[20]A. Abragam and B. Bleaney, *Electron Paramagnetic Resonance of Transition Ions* (Clarendon, Oxford, 1970).
[21]L. L. Hirst, Z. Phys. 244, 230 (1971).
[22]K. Wilson, Rev. Mod. Phys. 47, 773 (1975).
[23]L. L. Hirst, Int. J. Magn. 2, 213 (1972).
[24]A. Narath, Crit. Rev. Solid State Sci. 3, 1 (1972).
[25]J. B. Boyce, Ph.D. thesis (University of Illinois, 1972) (unpublished).
[26]C. M. Hurd, J. Phys. Chem. Solids 30, 539 (1968).
[27]E. C. Hirschkoff, O. G. Symko, and J. C. Wheatley, J. Low Temp. Phys. 5, 155 (1971).
[28]D. Davidov, C. Rettori, R. Orbach, A. Dixon, and E. P. Chock, Phys. Rev. B 11, 3546 (1975).
[29]M. Vochten, M. Labro, and S. Vynckier, Physica 86–88B, 467 (1977).
[30]H. G. Hoeve and D. O. Van Ostenburg, Phys. Rev. Lett. 26, 1020 (1971).
[31]P. Steiner, S. Hufner, and W. V. Zdrojewski, Phys. Rev. B 10, 4704 (1974).
[32]I. R. Williams, I. A. Campbell, C. J. Sanctuary, and G. V. H. Wilson, Solid State Commun. 8, 125 (1970).
[33]W. D. Brewer, Phys. Lett. 49A, 397 (1974).
[34]R. Ingalls, Phys. Rev. 133, A787 (1964).
[35]L. L. Hirst, Z. Phys. 245, 378 (1971).
[36]L. Azevedo, D. Follstaedt, and A. Narath, J. Appl. Phys. 50, 1746 (1979); the g value given in this reference is incorrect due to a computational error.
[37]L. Azevedo, D. Follstaedt, and A. Narath (private communication).
[38]S. Schultz and M. R. Shanabarger, Phys. Rev. Lett. 19, 749 (1967).
[39]P. Monod and S. Schultz, Phys. Rev. 173, 645 (1968).
[40]A. L. Ritter and R. H. Silsbee, Phys. Rev. B 17, 2833 (1978).
[41]H. Alloul and H. Ishii, J. Phys. (Paris) 22, L449 (1977).
[42]J. D. Cohen and C. P. Slichter, Phys. Rev. Lett. 40, 129, 483(E) (1978); Phys. Rev. B 22, 45 (1980).
[43]K. H. Johnson, D. D. Vredensky, and R. P. Messmer, Phys. Rev. B 19, 1519 (1979).
[44]C. P. Slichter, *Principles of Magnetic Resonance,* 2nd ed. (Springer-Verlag, New York, 1978).